

REPORT

# PEAK1 Y635 phosphorylation regulates cell migration through association with Tensin3 and integrins

Alba Zuidema<sup>1</sup>, Paul Atherton<sup>1</sup>, Maaïke Kreft<sup>1</sup>, Liesbeth Hoekman<sup>2</sup>, Onno B. Bleijerveld<sup>2</sup>, Nagarjuna Nagaraj<sup>3</sup>, Nanpeng Chen<sup>4</sup>, Reinhard Fässler<sup>4</sup>, and Arnoud Sonnenberg<sup>1</sup>

**Integrins mediate cell adhesion by connecting the extracellular matrix to the intracellular cytoskeleton and orchestrate signal transduction in response to chemical and mechanical stimuli by interacting with many cytoplasmic proteins. We used BioID to interrogate the interactomes of  $\beta 1$  and  $\beta 3$  integrins in epithelial cells and identified PEAK1 as an interactor of the RGD-binding integrins  $\alpha 5\beta 1$ ,  $\alpha V\beta 3$ , and  $\alpha V\beta 5$  in focal adhesions. We demonstrate that the interaction between integrins and PEAK1 occurs indirectly through Tensin3, requiring both the membrane-proximal NPxY motif on the integrin  $\beta$  tail and binding of the SH2 domain of Tensin3 to phosphorylated Tyr-635 on PEAK1. Phosphorylation of Tyr-635 is mediated by Src and regulates cell migration. Additionally, we found that Shc1 localizes in focal adhesions in a PEAK1 phosphorylated Tyr-1188-dependent fashion. Besides binding Shc1, PEAK1 also associates with a protein cluster that mediates late EGFR/Shc1 signaling. We propose a model in which PEAK1 binds Tensin3 and Shc1 to converge integrin and growth factor receptor signal transduction.**

## Introduction

Cell adhesion to the ECM is essential for the development and postnatal homeostasis of multicellular organisms. Cell-ECM adhesions are largely facilitated by the integrin family of adhesion receptors, which are formed through heterodimerization of an  $\alpha$  and  $\beta$  subunit. Depending on the combination of the 24  $\alpha$  and 8  $\beta$  subunits, integrins bind different ECM components, including laminins, collagens, and proteins containing an arginine (R), glycine (G), aspartic acid (D) tripeptide, such as fibronectin and vitronectin (Geiger and Yamada, 2011; Hynes, 2002). Integrins link the ECM to the intracellular cytoskeleton via a regulated network of adaptor proteins and recruit many cytoplasmic scaffolding and signaling proteins to generate an integrated signaling network with growth factor receptors (Morse et al., 2014). These protein complexes, known as the “integrin adhesome,” play key roles in a wide range of cellular processes, including cell migration, proliferation, differentiation, and survival. Failure to properly establish cell adhesion complexes can result in severe human diseases (Winograd-Katz et al., 2014).

Multiple studies have been undertaken to characterize the integrin adhesome and mechanistically understand how it drives a multitude of cellular functions in health and disease

(Horton et al., 2016; Manninen and Varjosalo, 2017). These efforts have resulted in an extensive literature-based adhesome protein-protein interaction network (Winograd-Katz et al., 2014; Zaidel-Bar et al., 2007), and a large list of adhesome components are a result of multiple proteomic studies (Manninen and Varjosalo, 2017). Combining different proteomic studies generated a dataset of 60 components termed the consensus integrin adhesome (Horton et al., 2015; Humphries et al., 2009; Ng et al., 2014; Robertson et al., 2015; Schiller et al., 2011; Schiller et al., 2013). Remarkably, only half of the proteins in the consensus adhesome are described in the literature-curated adhesome (Manninen and Varjosalo, 2017), indicating the need for further refinement.

A powerful technology to study protein interactions at nanometer resolution in integrin adhesion sites is the proximity-dependent biotin identification (BioID) assay combined with mass spectrometry (MS)-based proteomics (Roux et al., 2012). BioID has been used to characterize the proximity interactors of the focal adhesion (FA) proteins Paxillin and Kindlin2 (Dong et al., 2016) and to map the composition and topological features of integrin adhesion complexes by using 16 commonly

<sup>1</sup>Division of Cell Biology, The Netherlands Cancer Institute, Amsterdam, The Netherlands; <sup>2</sup>Proteomics Facility, The Netherlands Cancer Institute, Amsterdam, The Netherlands; <sup>3</sup>Mass Spectrometry Core Facility at the Max-Planck Institute of Biochemistry, Planegg, Germany; <sup>4</sup>Department of Molecular Medicine, Max-Planck Institute of Biochemistry, Planegg, Germany.

Correspondence to Arnoud Sonnenberg: [a.sonnenberg@nki.nl](mailto:a.sonnenberg@nki.nl).

© 2022 Zuidema et al. This article is distributed under the terms of an Attribution-Noncommercial-Share Alike-No Mirror Sites license for the first six months after the publication date (see <http://www.rupress.org/terms/>). After six months it is available under a Creative Commons License (Attribution-Noncommercial-Share Alike 4.0 International license, as described at <https://creativecommons.org/licenses/by-nc-sa/4.0/>).



identified adhesome components as bait (Chastney et al., 2020). Integration of these BioID datasets revealed a network of 147 proteins, of which only 11 were identified by multiple bait proteins and most likely represent the core adhesome components (Chastney et al., 2020). We also successfully used BioID to characterize the proximitome of integrin  $\beta 4$  and  $\beta 5$  in epithelial cells (Te Molder et al., 2020; Wang et al., 2020; Zuidema et al., 2018).

In the present study, we characterized the proximitome of integrin  $\beta 1$  and  $\beta 3$  and found a set of five adhesome components also reported in other BioID datasets (Chastney et al., 2020; Dong et al., 2016). Among the established integrin interactors Talin1, Kindlin2, and Tensin3, we also identified Kank2 and pseudopodium-enriched atypical kinase 1 (PEAK1; Sgk269). PEAK1 is a member of the PEAK family of pseudokinases, can form homo- or heterodimers with its family member inactive tyrosine-protein kinase PRAG1 (Skg223; Ha and Boggon, 2018; Patel et al., 2017; Patel et al., 2020), and associates with FAs and the EGFR signaling pathway (Bristow et al., 2013; Chastney et al., 2020; Dong et al., 2016; Wang et al., 2010; Zheng et al., 2013). How PEAK1 is integrated into FAs and whether it links FA and EGFR signaling is poorly understood. Several studies have reported elevated levels of PEAK1 and implicated PEAK1 in the regulation of tumor cell proliferation and invasion (Abu-Thuraia et al., 2020; Agajanian et al., 2015; Croucher et al., 2013; Ding et al., 2018; Fujimura et al., 2014; Kelber et al., 2012; Strnad et al., 2017). Furthermore, it was shown that PEAK1 is phosphorylated by Src family kinases downstream of growth factor receptors, which promotes its localization in FAs (Agajanian et al., 2015; Bristow et al., 2013; Leroy et al., 2009; Wang et al., 2010; Zheng et al., 2013). PEAK1 also interacts with the scaffolding protein Shc1, which occurs upon EGF stimulation with a delayed kinetics and regulates the assembly of a protein cluster involved in cytoskeletal reorganization (Zheng et al., 2013). Finally, PEAK1 has been identified as a component of the canonical Src-p130Cas-CrkII-Paxillin and Erk signaling pathways (Wang et al., 2010). Our findings show that PEAK1 is a specific proximity interactor of RGD-binding integrins in FAs, and that phosphorylation of Tyr-635 in PEAK1 regulates cell migration through association with Tensin3. In turn, PEAK1 recruits Shc1 to FAs, which increases Shc1 phosphorylation and thereby links the integrin adhesion and EGFR signaling pathways.

## Results

### Identification of PEAK1 as core FA component

To characterize the integrin  $\beta 1$  and  $\beta 3$  proximitome by BioID (Fig. 1 A), we transfected  $\beta 1$ -null mouse epithelial GE11 cells (Gimond et al., 1999) with integrin  $\beta 1$ - or  $\beta 3$ -BirA\* cDNA and selected the bulk population of cells expressing the integrin-BirA\* fusion proteins by FACS. Integrin  $\beta 1$ - and  $\beta 3$ -BirA\* localized in FAs and  $\beta 1$ -BirA\* additionally in cell-cell contacts and in adhesion structures that resemble fibrillar adhesions/podosomes (Fig. 1 B). Cells were treated for 24 h with biotin before cell lysis, and untreated cells were used as negative controls. The use of untreated controls allowed us to normalize for any changes in protein composition resulting from expression of integrin  $\beta 1$  or

$\beta 3$ . Purified proteins were run and excised from a stained polyacrylamide gel and analyzed by LC-MS/MS. We cannot rule out that the C-terminal fusion of the BirA\* to the cytoplasmic tail of integrin  $\beta 1$  or  $\beta 3$  could interfere with the recruitment of some integrin-associated proteins; nevertheless this approach resulted in datasets of 170 and 61 proteins for  $\beta 1$  and  $\beta 3$ , respectively (Fig. 1, C and D; Fig. S1; and Tables S1, S2, S3, and S4). Among the top integrin proximity interactors, we found the integrin-binding proteins Talin1/2, Kindlin2, and Tensin3. Furthermore, PEAK1 and Kank2 were also among the significantly enriched proteins (Fig. 1, C and D). Major differences between the  $\beta 1$  and  $\beta 3$  proximitomes were the integrin  $\alpha$  subunits ( $\alpha 2$ ,  $\alpha 3$ ,  $\alpha 5$ ,  $\alpha 6$ , and  $\alpha 7$  for  $\beta 1$  and  $\alpha V$  for  $\beta 3$ ) and the enrichment of CD151 in the proximity of  $\beta 1$  (Fig. 1 E). Further comparison of the  $\beta 1$  and  $\beta 3$  datasets revealed a common set of 46 proteins (Figs. 1 F and S1 A), which was further compared to the proximitomes of Paxillin and Kindlin2 (Dong et al., 2016) revealing an overlap with 6 adhesome components (Fig. 1 F). Among them were proteins associated with FAs (Talin1, Kindlin2, and Tensin3) and the cortical microtubule stabilizing complex (Kank2; Bouchet et al., 2016; Sun et al., 2016). Additionally, PEAK1 and EphA2 were identified in all four datasets. Talin1, Tensin3, Kank2, and PEAK1 were also identified by Chastney et al. (2020) using multiple FA proteins, including Kindlin2, as bait. Whereas Talin1 and Kindlin2 were reported in both the consensus adhesome (Horton et al., 2015) and the literature-curated adhesome ([www.adhesome.org](http://www.adhesome.org); Winograd-Katz et al., 2014; Zaidel-Bar et al., 2007), Tensin3 was reported only in the consensus adhesome, PEAK1 in the literature-curated dataset, and EphA2 and Kank2 in neither (Fig. 1 E).

The identification of Talin1, Kindlin2, Tensin3, Kank2, and PEAK1 as adhesome components in multiple studies, together with their close association to integrin  $\beta 1$  and  $\beta 3$  observed in our experiments, points to their crucial role in integrin function. Because the interaction between PEAK1 and integrins is poorly understood, we decided to study this interaction.

### PEAK1 interacts with RGD-binding integrins

Cell adhesion to fibronectin was shown to induce PEAK1 tyrosine phosphorylation (Wang et al., 2010). The fibronectin dependence of this process suggests that PEAK1 associates with RGD-binding integrins. Immunofluorescence analysis of endogenous PEAK1 (Fig. 2 A) or overexpression of PEAK1-GFP (Fig. 2 B) in GE11/ $\beta 1$ -BirA\* cells shows that the protein localized to cell matrix adhesions.

Integrin  $\alpha V\beta 3$  is a receptor for RGD-containing ECM proteins, but  $\beta 1$  can heterodimerize with 12 different  $\alpha$  subunits to additionally mediate adhesion to laminins and collagens. To study the specificity of the integrin-PEAK1 interaction, we overexpressed integrin  $\alpha 3$ -,  $\alpha 5$ -, or  $\alpha 6$ -BirA\* fusion proteins in GE11 cells that also stably express integrin  $\beta 1$ . These integrin  $\alpha$  subunits are expressed at high levels in GE11 cells and are among the top hits in the  $\beta 1$  proximitome (Fig. 1 C). All overexpressed integrin  $\alpha$  BirA\* constructs were expressed at the cell surface and similar levels of Itg.  $\beta 1$  could be detected using FACS analysis (Fig. S1 B). Integrin  $\alpha 3\beta 1$  and  $\alpha 6\beta 1$  are laminin receptors, whereas  $\alpha 5\beta 1$  binds fibronectin. Overexpression of the  $\alpha$  subunits resulted in an altered  $\beta 1$  subcellular distribution, with

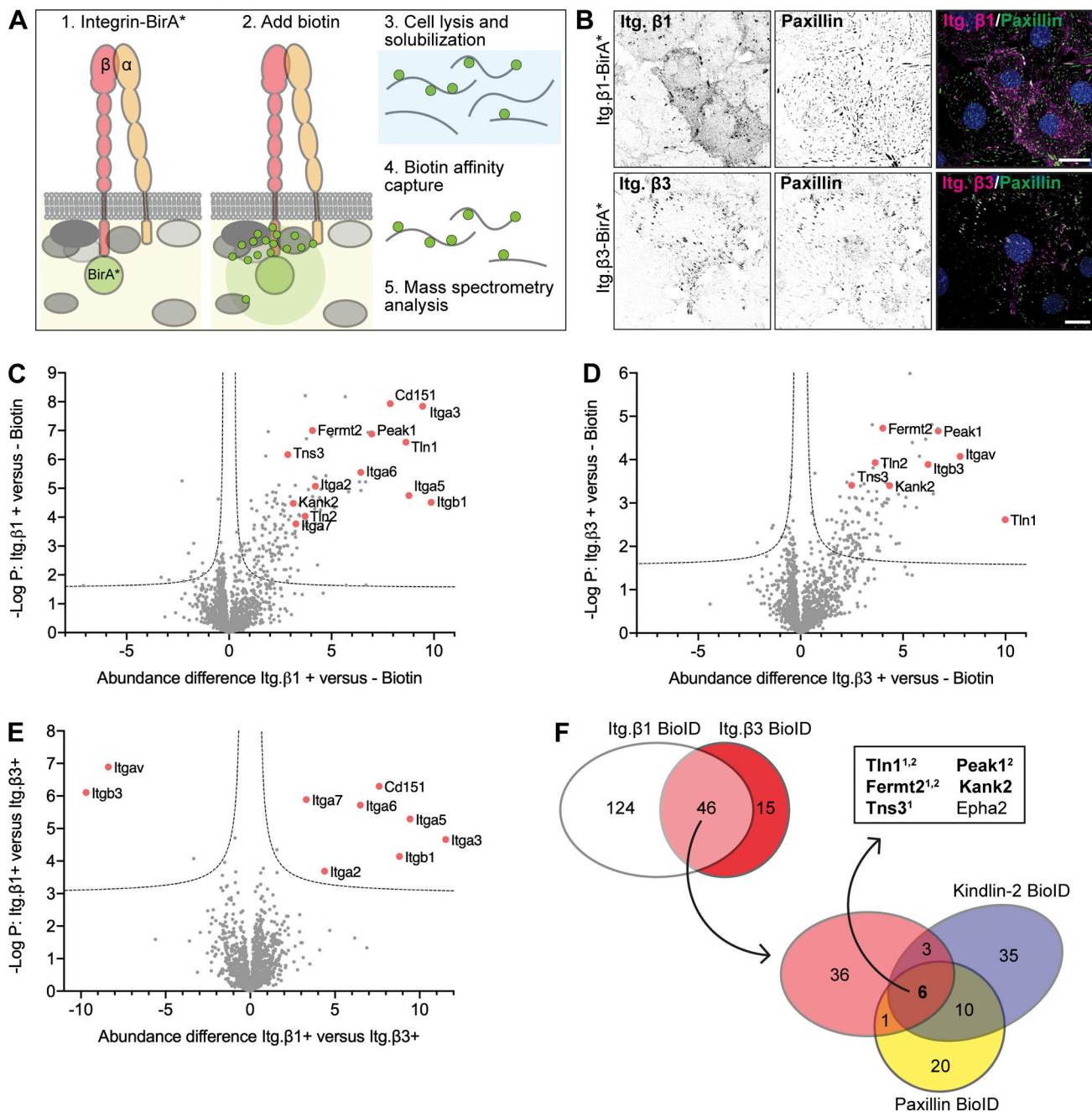


**Figure 1. Identification of PEAK1 as a proximity interactor of integrin  $\beta$ 1 and  $\beta$ 3.** (A) Schematic depiction of the BioID assay. Integrin  $\beta$  subunits are tagged with the promiscuous biotin ligase BirA\* on the cytoplasmic domain. Biotin is added to allow biotinylation of neighboring proteins, which are identified by MS analysis after cell lysis and isolation of biotinylated proteins using streptavidin beads. (B) Integrin  $\beta$ 1- or  $\beta$ 3-BirA\* was expressed in  $\beta$ 1-null GE11 cells and visualized using antibodies against the  $\beta$ 1 or  $\beta$ 3 subunit (magenta in merge). FAs (stained with phospho-Y31 Paxillin) are shown in green, and nuclei (stained with DAPI) in blue. Scale bar, 20  $\mu$ m. (C and D) MS analysis of proximity interactors of  $\beta$ 1 (C) and  $\beta$ 3 (D). Cells were lysed after 24 h of 50  $\mu$ M biotin treatment. Untreated cells were used as negative control. Volcano plot shows proteins enriched in biotin-treated over control samples. The logarithmic ratio of protein LFQs were plotted against negative logarithmic P values of a two-sided two-sample t test. The hyperbolic curve separates significantly enriched proteins from common binders (FDR: 0.05,  $n = 4$ ). (E) Volcano plot shows the proximity interactors of  $\beta$ 1 versus  $\beta$ 3 for samples treated with biotin. (F) Comparison of the proximity interactors of  $\beta$ 1/3 and Kindlin2/Paxillin (Dong et al., 2016) results in six proteins found in all datasets. Of these six proteins, five are also identified in the integrin adhesome BioID study of Chastney et al. (2020) (bold font). 1, mentioned in consensus adhesome (Horton et al., 2015); 2, www.adhesome.org.

$\beta$ 1 localizing in FAs in the  $\alpha$ 5-BirA\*-expressing cells and showing a more dispersed organization in the  $\alpha$ 3- and  $\alpha$ 6-BirA\*-expressing cells (Fig. 2 C), likely owing to the ability of integrin  $\alpha$ 3 $\beta$ 1 and  $\alpha$ 6 $\beta$ 1, but not  $\alpha$ 5 $\beta$ 1, to incorporate into

tetraspanin webs through their interaction with CD151 (Charrin et al., 2014).

To examine whether PEAK1 associates primarily with the RGD-binding  $\alpha$ 5 $\beta$ 1 integrin, we performed BioID assays combined

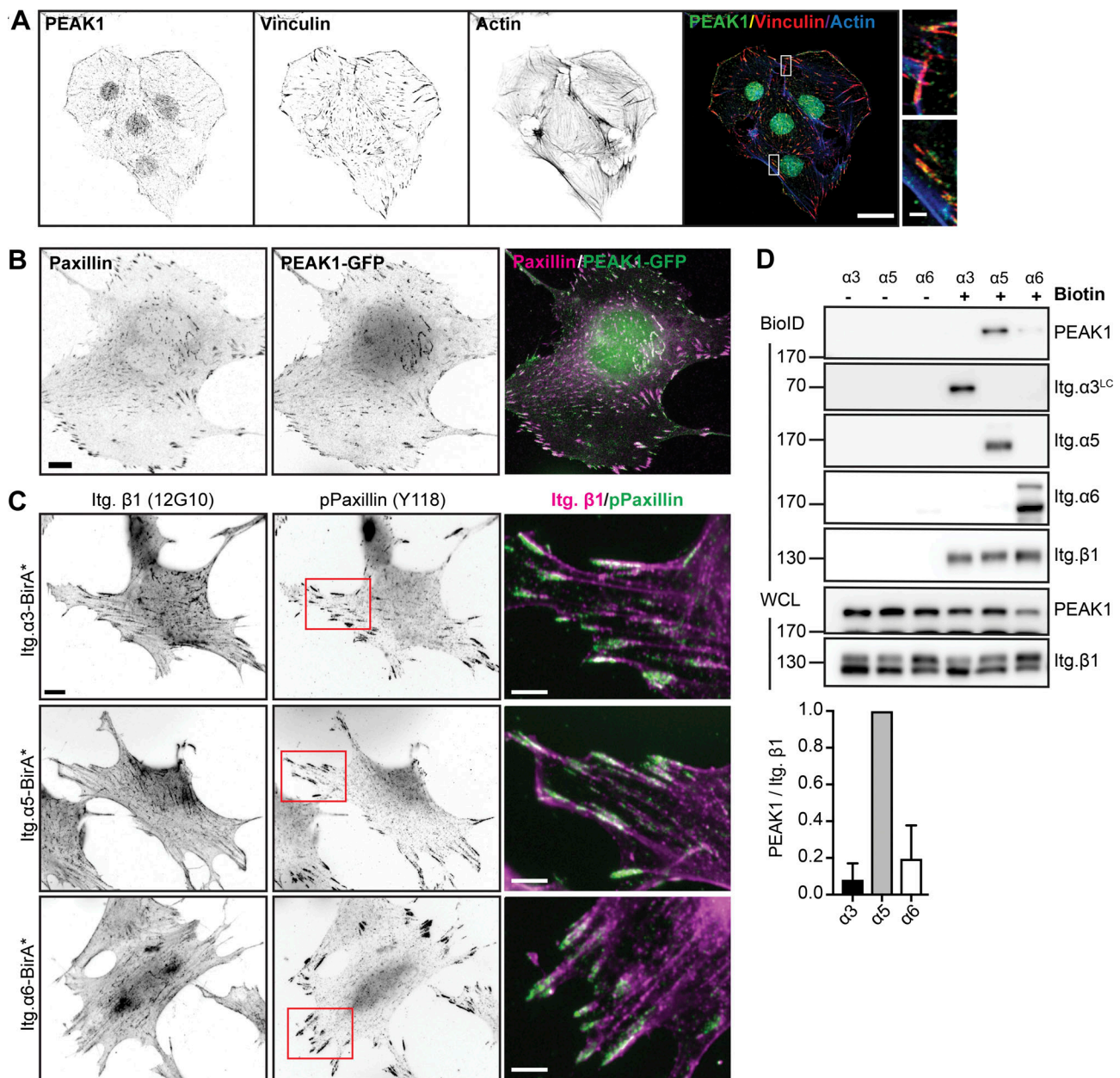


**Figure 2. PEA1 interacts with integrin  $\alpha$ 5 $\beta$ 1.** (A) Immunofluorescence analysis of PEA1 (green in merge), vinculin (red in merge), and actin (blue in merge) in GE11 cells expressing  $\beta$ 1-BirA\*. Nuclear localization of PEA1 is not specific. Scale bar, 20  $\mu$ m; in magnified region, 2  $\mu$ m. (B) Overexpression of PEA1 in GE11 Tet-ON integrin  $\beta$ 1 cells treated with 1  $\mu$ g/ml doxycycline for 48 h to induce  $\beta$ 1 expression. Scale bar, 20  $\mu$ m. (C) Integrin  $\alpha$ 3-,  $\alpha$ 5-, or  $\alpha$ 6-BirA\* was expressed in GE11 cells that stably express  $\beta$ 1. Subcellular distribution of (active)  $\beta$ 1 (12G10 antibody; magenta in merge) together with Paxillin (Y118) is shown. Scale bar, 10  $\mu$ m; scale bar in magnified regions, 5  $\mu$ m. (D) Representative Western blots of the BioID assays performed using the GE11/ $\beta$ 1 cells expressing the integrin  $\alpha$ 3-,  $\alpha$ 5-, or  $\alpha$ 6-BirA\* shown in C. Cells were grown to subconfluence in plastic tissue culture plates and treated with 50  $\mu$ M biotin for 24 h before cell lysis. Quantifications of PEA1 signal intensities normalized to integrin  $\beta$ 1 levels are shown ( $n = 3$ ; bars show mean with SD). Source data are available for this figure: SourceData F2.

with Western blot analysis to determine the levels of biotinylated PEA1 in GE11 cells stably expressing integrin  $\beta$ 1 and overexpressing integrin  $\alpha$ 3-,  $\alpha$ 5-, or  $\alpha$ 6-BirA\* fusion proteins. Strong biotinylation of PEA1 was detected in cells expressing  $\alpha$ 5-BirA\* but was absent or hardly detected in cells expressing the  $\alpha$ 3- or  $\alpha$ 6-BirA\* constructs (Fig. 2 D). Altogether, these findings demonstrate that PEA1 localizes in FAs and acts downstream of the RGD-binding integrins  $\alpha$ 5 $\beta$ 1 and  $\alpha$ V $\beta$ 3.

### Tensin3 links PEA1 and integrins

Many adaptor proteins engage with the conserved membrane-proximal (MP) NPxY or membrane-distal (MD) NxxY motifs on the cytoplasmic tail of integrin  $\beta$  subunits (Calderwood et al., 2003). For example, the MP-NPxY is required for the interaction of Talin1 with the integrin  $\beta$ 1/3 subunit, while the MD-NxxY motif is needed for Kindlin2 binding (Moser et al., 2009). PEA1 does not contain an integrin-binding FERM or PTB

domain found in other proteins that interact with the MP-NPXY or MD-NxxY motifs (Wang et al., 2010). Therefore, we hypothesized that the interaction between PEA1 and integrin  $\beta$  subunits might be indirect, through an adaptor protein. To further examine the PEA1-integrin interaction, we generated  $\beta$ 1- and  $\beta$ 3-BirA\* fusion proteins carrying disruptive Y>A mutations in the MP-NPXY (termed N1), MD-NxxY (termed N2), or both (termed N1 + 2; Fig. 3 A). These mutants were stably expressed in  $\beta$ 1-null GE11 cells; FACS analysis confirmed that all the mutants were expressed at the cell surface at similar levels (Fig. S1 C). The generated cell lines were used to perform BioID combined with MS (Fig. 3, B and C). Our experiments revealed that the proximity of Talin, Tensin3, and PEA1 to  $\beta$ 1/3 was strongly impaired when MP-NPXY was mutated and reduced when MD-NPXY was mutated. These results were confirmed by performing BioID assays in combination with Western blot analysis (Fig. 3, D and E).

To determine which integrin MP-NPXY motif interacting protein could mediate the PEA1-integrin association, we depleted established interactors of the integrin MP-NPXY motif by using siRNAs and studied the effects on the integrin-PEA1 interaction by BioID and Western blot. Interestingly, knock-down of Talin1/2 or Filamins (Calderwood et al., 2003; Kiema et al., 2006) did not reduce the integrin  $\beta$ 1-PEA1 proximity interaction (Fig. S2 D). We therefore wondered whether the proximity interaction between RGD-binding integrins and PEA1 could be mediated by Tensin3, which contains a C-terminal PTB domain shown to interact with the integrin MP-NPXY domain (Calderwood et al., 2003; McCleverty et al., 2007) and was identified as an interactor of  $\beta$ 1 and  $\beta$ 3 in our proximity screen (Figs. 1 and 3). Unfortunately, we were unable to successfully reduce Tensin3 expression by using siRNAs/shRNAs or CRISPR/Cas9-mediated gene disruption in GE11 cells. As an alternative approach to investigate whether Tensin3 mediates the integrin-PEA1 association, we generated PEA1-deficient GE11/ $\beta$ 1-BirA\* cells using CRISPR/Cas9 and subsequently introduced WT or mutant forms of PEA1 that carried a Y635F or Y1188F substitution. The Y635F mutation was selected based on the remarkable similarity of the <sup>635</sup>YDNL sequence in PEA1 to the YDNL sequence present in DLC1, which mediates an interaction with the Tensin SH2 domain that precedes the PTB domain (Liao et al., 2007; Yam et al., 2006). Moreover, YDNL was identified as a binding peptide motif in a pY peptide library screen using the SH2 domain of Tensin (Wavreille and Pei, 2007). On the other hand, Y1188 was shown to bind Shc1, which could represent an alternative connection between PEA1 and the integrin  $\beta$  NPXY motif (Cowan et al., 2000; Deshmukh et al., 2010; Smith et al., 2006; Zheng et al., 2013). BioID experiments combined with Western blot analysis clearly indicated that phosphorylation of Y635 in PEA1 establishes the proximity interaction with integrin  $\beta$ 1, while Shc1 binding is not required for the PEA1- $\beta$ 1 interaction (Fig. 4, A and B).

### PEA1 binds to Tensin3 in a phosphorylation-dependent manner to connect to integrins

To demonstrate that PEA1 interacts directly with Tensin3 in a phosphorylation-specific manner, we expressed GFP-tagged

PEA1 or PEA1-Y635F in CRISPR/Cas9-generated PEA1-knockout human colorectal SW480 cells (Fig. S2 A). GFP-PEA1 was expressed at high levels and used for GFP pull-down experiments. Cells were serum-starved overnight and treated with pervanadate, an irreversible inhibitor of protein tyrosine phosphatases, before lysis. GFP pull-down experiments showed that Tensin3 is associated with PEA1 in pervanadate-treated samples but hardly associated with PEA1 in serum-starved PEA1-WT- or PEA1-Y635F-expressing cells (Fig. 4, C and D). Furthermore, PEA1-Y635F showed reduced colocalization with Tensin3 compared with PEA1-WT (Fig. S2 B). Intriguingly, the interaction between DLC1 and the SH2 domain of Tensin3/c-ten does not require phosphorylation of the YDNL motif in DLC1 (Cao et al., 2015; Liao et al., 2007) and is less dependent on the tyrosine phosphorylation of the Tensin3 SH2 domain (Qian et al., 2009). This indicates that direct competition between DLC1 and PEA1 for Tensin3 binding is unlikely, because phosphorylation events upon growth factor stimulation would promote a switch from Tensin3-DLC1 to Tensin3-PEA1 binding (Chumbalkar et al., 2011; Cui et al., 2004).

PEA1 is recruited to FAs upon phosphorylation by Src family kinases (Bristow et al., 2013; Croucher et al., 2013; Leroy et al., 2009; Wang et al., 2010). In GE11 cells, where Src is already maximally active in the absence of EGF stimulation (i.e., its activity cannot be further increased by EGF stimulation; Fig. S2 C), PEA1 is highly phosphorylated on Y635 (Fig. S2 D). To analyze whether PEA1 phosphorylation by Src is required for the PEA1-Tensin3- $\beta$ 1 interaction, we conducted a BioID assay using GE11/ $\beta$ 1-BirA\* cells treated with Saracatinib, an inhibitor of Src and Abl family kinases. Saracatinib treatment decreased tyrosine phosphorylation of PEA1 and decreased the proximity interaction between PEA1 and  $\beta$ 1 (Fig. S2 E), in line with previous findings (Bristow et al., 2013). GFP pull-down experiments using PEA1-deficient GE11 cells expressing GFP-PEA1 treated with Saracatinib confirmed that phosphorylation of PEA1-Y635 is decreased upon Src inhibition (Fig. S2 F).

Notably, Src has also been implicated in the phosphorylation of the SH2 domain of Tensin3, and tyrosine phosphorylation of the SH2 domain contributes to complex formation with several proteins (Qian et al., 2009). To determine the importance of tyrosine phosphorylation of the SH2 domain for PEA1 binding, we transiently expressed SH2-WT and SH2 double (SH2-2F; Y1206 and Y1256F) and SH2 triple (SH2-3F; Y1173F, Y1206, and Y1256F) mutants, engineered as GST fusion proteins together with PEA1 in COS-7 cells. Cells were treated or not with pervanadate for 10 min. GST pull-down confirmed that the Tensin3 SH2-WT binds to PEA1 and showed that tyrosine phosphorylation of the SH2 domain greatly enhanced the binding of Tensin3 to PEA1 (Fig. 4 E). Compared with Tensin3 SH2-WT, binding of the SH2-2F mutant to PEA1 was only slightly reduced, but that of the SH2-3F mutant was reduced by >50% (Fig. 4, E and F).

Next, we analyzed the PEA1-Tensin3-integrin interaction in human U251MG glioblastoma cells, which express Tensin3 at high levels. PEA1 and Tensin3 colocalized in FAs, as shown by immunofluorescence analysis (Fig. 4 G). In line with our biochemistry results, PEA1 was absent from cell matrix adhesions

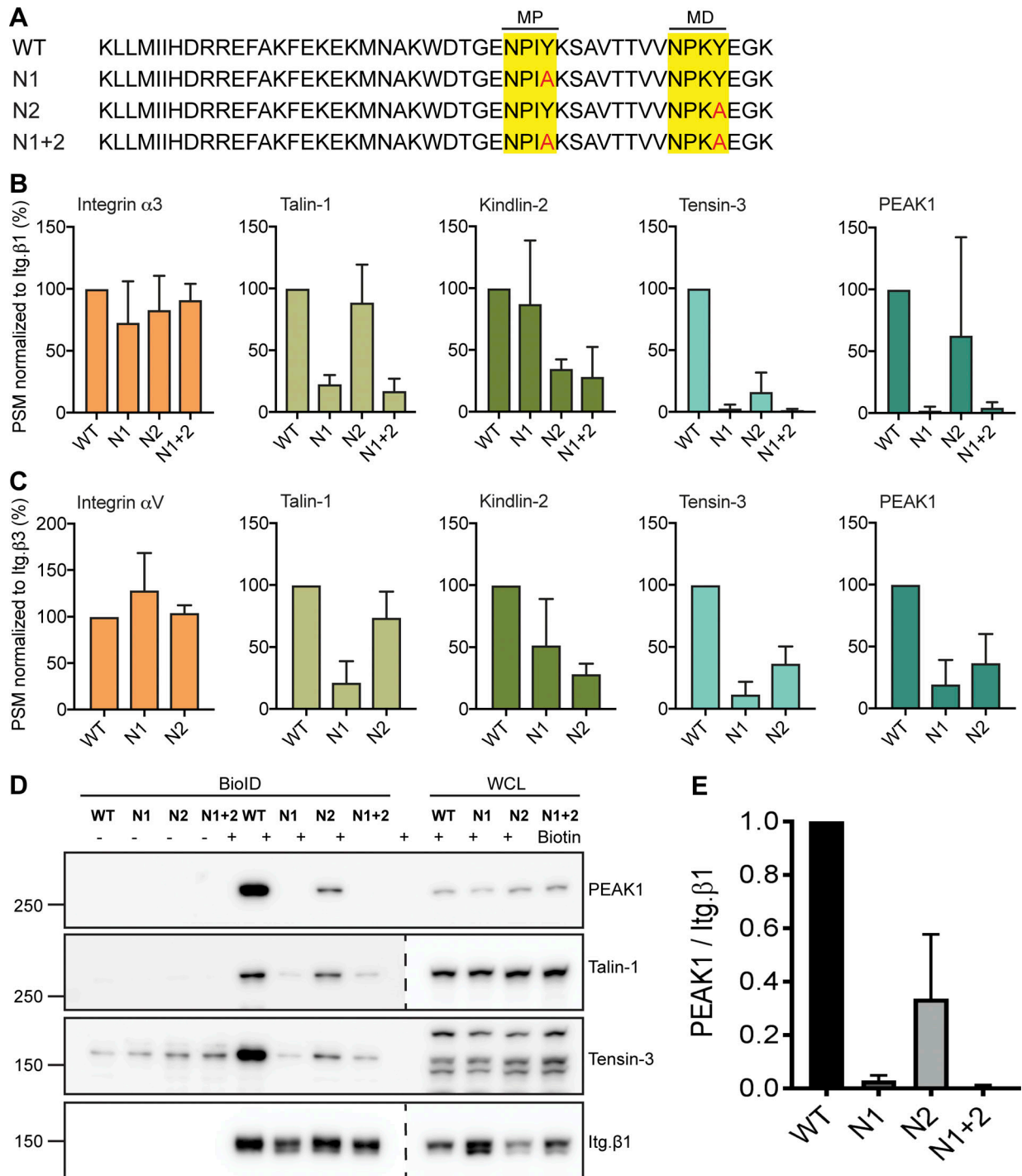


Figure 3. **Integrin  $\beta$ 1 and  $\beta$ 3 MP-NPXY motif required for interaction with PEAK1.** (A) Amino acid sequence of integrin  $\beta$ 1 cytoplasmic domain and  $\beta$ 1 mutants that contain Y>A mutations in the MP and/or MD NPXY motifs. (B and C) Peptide spectral match (PSM) values of selected proximity interactors of  $\beta$ 1 (B) and  $\beta$ 3 (C) WT and NPXY/NxxY mutants as analyzed by MS. PSM values are normalized to the PSM values of the integrin-BirA\* fusion protein ( $n = 3$ ; bars show mean with SD). (D) Validation by Western blot of the experiments shown in B and C. WCL, whole-cell lysate. (E) Quantifications of PEAK1 signal intensities normalized to integrin  $\beta$ 1 levels are shown ( $n = 3$ ; bars show mean with SD). Source data are available for this figure: SourceData F3.

in U251MG cells spread on fibronectin in the presence of the Src inhibitor Saracatinib (Fig. S2 G). Integrin  $\alpha$ V $\beta$ 5 is the main RGD-binding integrin found to colocalize with Tensin3 and PEAK1 in FAs, whereas integrin  $\beta$ 1 shows a more dispersed subcellular distribution, and integrin  $\beta$ 3 could not be detected (Fig. 4 G). We

performed BioID assays by expressing  $\beta$ 5-BirA\* in  $\beta$ 5-deficient U251MG cells that were additionally depleted of Tensin3 by shRNA-mediated gene knockdown. Depletion of Tensin3 by two different shRNAs reduced the PEAK1-integrin  $\beta$ 5 proximity interaction (Fig. 4, H and I), while the Talin1-integrin  $\beta$ 5

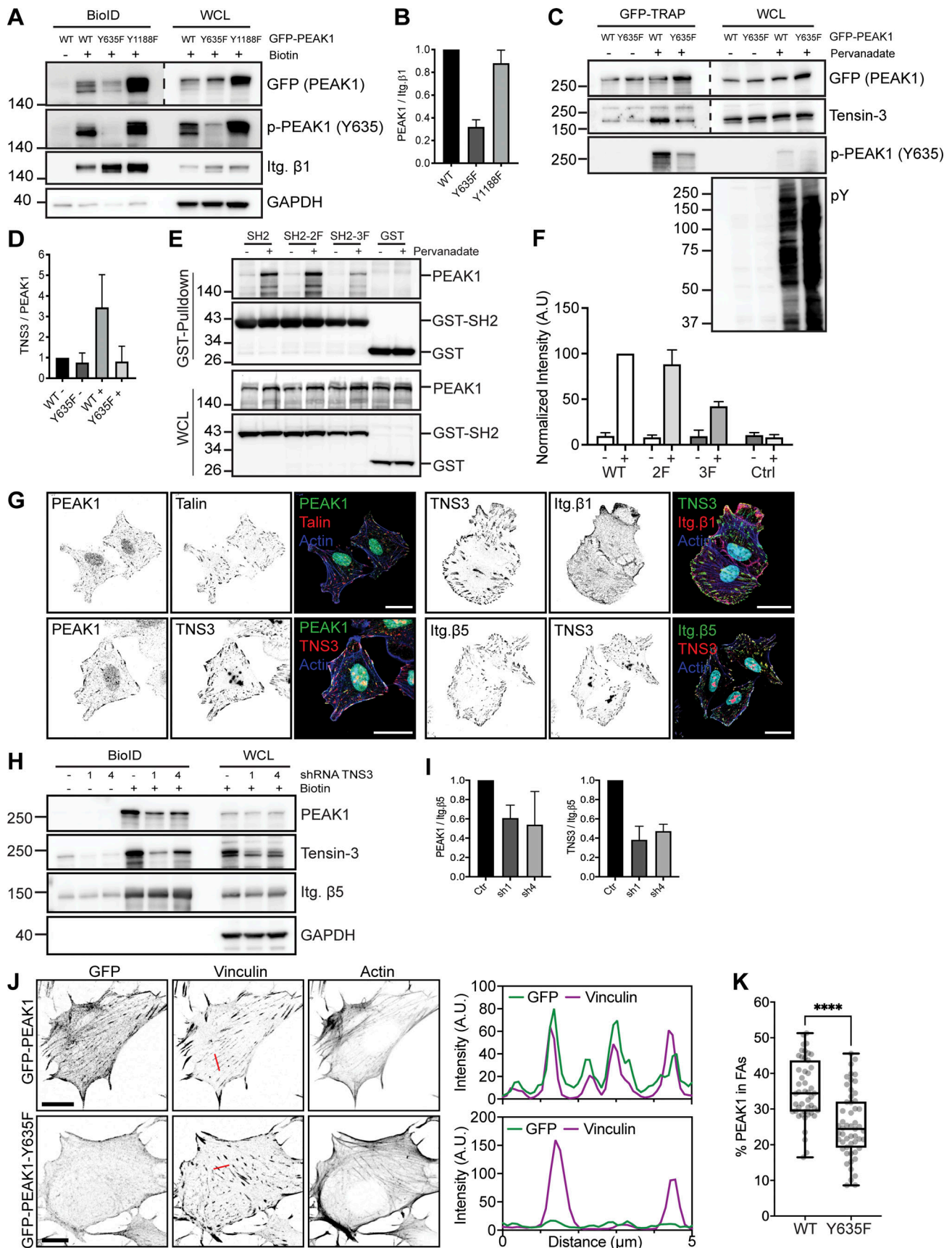


Figure 4. **Tensin3 binds to p-Y635 PEAK1.** (A) Integrin  $\beta 1$ -BirA\* and GFP-PEAK1 WT or Y635F/Y1188F mutants were expressed in PEAK1-deficient GE11 cells. Representative Western blots of BioID assays are shown. (B) Quantifications of PEAK1 signal intensities normalized to integrin  $\beta 1$  levels are shown ( $n = 3$ ; bars

show mean with SD). **(C)** GFP-PEAK1 WT and Y635F mutant were expressed in PEAK1-deficient SW480 cells. Cells were serum starved overnight and then treated with pervanadate for 10 min before cell lysis. Representative Western blots are shown of GFP-TRAP experiments. WCL, whole-cell lysate. **(D)** Quantification of Tensin3 signal intensities normalized to PEAK1 (GFP) levels are shown ( $n = 3$ ; bars show mean with SD). **(E)** COS-7 cells transiently transfected with GST and GST-SH2 constructs together with a plasmid expressing HA-tagged full-length PEAK1 were treated with or without pervanadate for 10 min. Cell lysates derived from these transfected cells were subjected to a GST pull-down assay with glutathione-Sepharose (GE Healthcare). WCLs and the pulled-down proteins were analyzed by Western blotting with antibodies against PEAK1 (D4G6) and GST (2F3). **(F)** Quantification of Tensin3 signal intensities normalized to those of GST are shown ( $n = 3$ ; bars show mean with SD). **(G)** Colocalization of PEAK1, Talin, Tensin3, and integrin  $\beta 1$  and  $\beta 5$  (shown in green or red in merge) in U251MG cells seeded on glass coverslips and cultured in medium supplemented with 10% FCS. Actin cytoskeleton (blue) and nuclei (cyan) are visualized. Scale bar, 20  $\mu\text{m}$ . **(H)** Representative Western blots of BioID assays performed using integrin  $\beta 5$ -deficient U251MG cells expressing  $\beta 5$ -BirA\*, in which Tensin3 was depleted by two different shRNAs (1 and 4). Cells were treated with 50  $\mu\text{M}$  biotin 24 h before cell lysis. **(I)** Quantifications of PEAK1 and Tensin3 signal intensities normalized to integrin  $\beta 5$  levels are shown ( $n = 3$ ; bars show mean with SD) in I. **(J)** Colocalization of vinculin and GFP-PEAK1 WT versus Y635F in PEAK1-deficient GE11 tet-ON integrin  $\beta 1$  cells treated with 1  $\mu\text{g}/\text{ml}$  doxycycline for 48 h to induce  $\beta 1$  expression. Scale bar, 10  $\mu\text{m}$ . **(K)** Quantifications of colocalization of FAs and PEAK1 (calculated as a percentage of total PEAK1) of immunofluorescence images as shown in K. FAs were stained with vinculin or pY.  $n = 3$ ; total number of cells analyzed: 47 (WT); 53 (Y635F). Box plots range from the 25th to 75th percentile; central line indicates the median; whiskers show smallest to largest value. Mann-Whitney  $U$  test was performed to determine statistical significance. \*\*\*\*,  $P < 0.0001$ . Source data are available for this figure: SourceData F4.

interaction was not affected (Fig. S2 H). Furthermore, PEAK1 was absent from cell matrix adhesions in Tensin3-depleted cells (Fig. S2 I). Finally, we compared the localization of GFP-PEAK1 WT versus Y635F in FAs by immunofluorescence analysis. PEAK1-Y635F showed significantly reduced colocalization with the FA marker Vinculin compared with WT PEAK1 (Fig. 4, J and K). Taken together, these results indicate that Src-mediated phosphorylation of PEAK1 and the SH2 domain of Tensin3 promote their binding and facilitate PEAK1 interaction with the integrin  $\beta$  MP-NPXY motif.

### Mapping the PEAK1 interactome

To identify additional proteins that interact with PEAK1, we used a GFP-Trap-based affinity purification method combined with MS using PEAK1-deficient GE11 cells that express GFP-PEAK1, or the PEAK1-deficient cells as a negative control. This screen identified Shc1 and many proteins involved in the EGFR/Shc1 signaling network (Zheng et al., 2013), including Asap1/2, Dab2ip, Grb2, Lrrk1, Ppp1ca/cc, Prag1, and Rasal2 as major PEAK1 interacting proteins (Fig. 5 A and Table S5). Both human and mouse PEAK1 were enriched in the GFP-PEAK1 sample, indicating that endogenous PEAK1 is not completely deleted in our GE11 control sample and dimerizes with the GFP-PEAK1 fusion protein (Patel et al., 2020). Tensin3 was not found as a significant interactor of PEAK1 in this analysis (Fig. 5 A). However, in a GFP-Trap pull-down assay using SW480 cells, a physical interaction between Tensin3 and PEAK1 could be demonstrated and was found to be dependent on the phosphorylation of PEAK1 at Y635 (Fig. 4 C). Interestingly, Asap1/2 and Grb2 were recently identified as binding partners of the smaller PEAK family member PEAK3 (Hou et al., 2022), suggesting that these proteins may interact with conserved domains in PEAK1-3.

Because PEAK1 is a scaffolding protein that functions in late EGFR-mediated signaling responses (Zheng et al., 2013), we investigated whether the PEAK1 interactome changes upon 20-min EGF stimulation. The major interactors of PEAK1 remained unchanged after EGF treatment (Fig. S3), which is in line with our finding that Src is already maximally phosphorylated and PEAK1 phosphorylation is high in GE11 cells. However, Ptpn13 and Shroom2 were identified as additional, EGF-induced PEAK1-binding proteins (Fig. S3). The interaction

of these proteins with PEAK1 likely depends on non-Src-mediated posttranslational modifications that occur downstream of EGFR activation.

To further analyze the scaffolding function of PEAK1, we expressed different PEAK1 mutants in PEAK1-depleted GE11 cells and subsequently performed GFP pull-down experiments. Western blot analysis indicated that the Y1188F mutation almost completely abrogated the binding of PEAK1 to Shc1, but not to Rasal2 and only slightly to Grb2 (Fig. 5 B). Grb2 binding to PEAK1-Y635E/F decreased by  $\sim 50\%$ , whereas Shc1 was unchanged. Interestingly, however, binding of tyrosine-phosphorylated Shc1 to PEAK1-Y635E/F was strongly decreased (Fig. 5 B). In line with these biochemical findings, immunofluorescence analysis revealed that PEAK1 recruits Shc1 to FAs (Fig. 5 C). Recruitment of Shc1 to FAs in PEAK1-deficient or PEAK1-Y1188F mutant cells shown by colocalization with phospho-Paxillin was significantly reduced (Fig. 5, C and D). Because PEAK1-Y635F cannot bind Tensin3, we speculate that the phosphorylation of Shc1 is increased upon its recruitment to FAs, via PEAK1-Tensin3-integrin binding. Grb2, which also binds PEAK1-Y635, is not found in FAs and therefore does not play a major role in the localization and phosphorylation of Shc1 in FAs. In line with our findings, Shc1 interacts with the FA-forming integrins, including  $\alpha 5\beta 1$  and  $\alpha V\beta 3$ , and is phosphorylated by integrin  $\beta 1$  crosslinking or when cells are plated on fibronectin/vitronectin (Wary et al., 1996). Shc1 controls various cellular processes in association with integrins and growth factor stimulation, including cell survival, proliferation, and migration (Mauro et al., 1999; Wary et al., 1996). Therefore, we tested the contribution of PEAK1 phosphorylation at either Y635 or Y1188 to cell motility. GE11 cells depleted of endogenous PEAK1 migrated  $\sim 40\%$  more slowly compared with WT GE11 cells; reexpression of PEAK1-GFP was able to rescue this reduction in cell velocity (Fig. 5 E). The motility defect of the PEAK1-depleted GE11 cells was also rescued by expression of PEAK1-Y1188F-GFP, but not PEAK1-Y635F-GFP (Fig. 5 E).

### Conclusions

We report here that Tensin3 mediates the proximity interaction between PEAK1 and RGD-binding integrins through binding of its SH2 domain to PEAK1. Our findings indicate that PEAK1 mainly interacts with Shc1 and its associated protein cluster

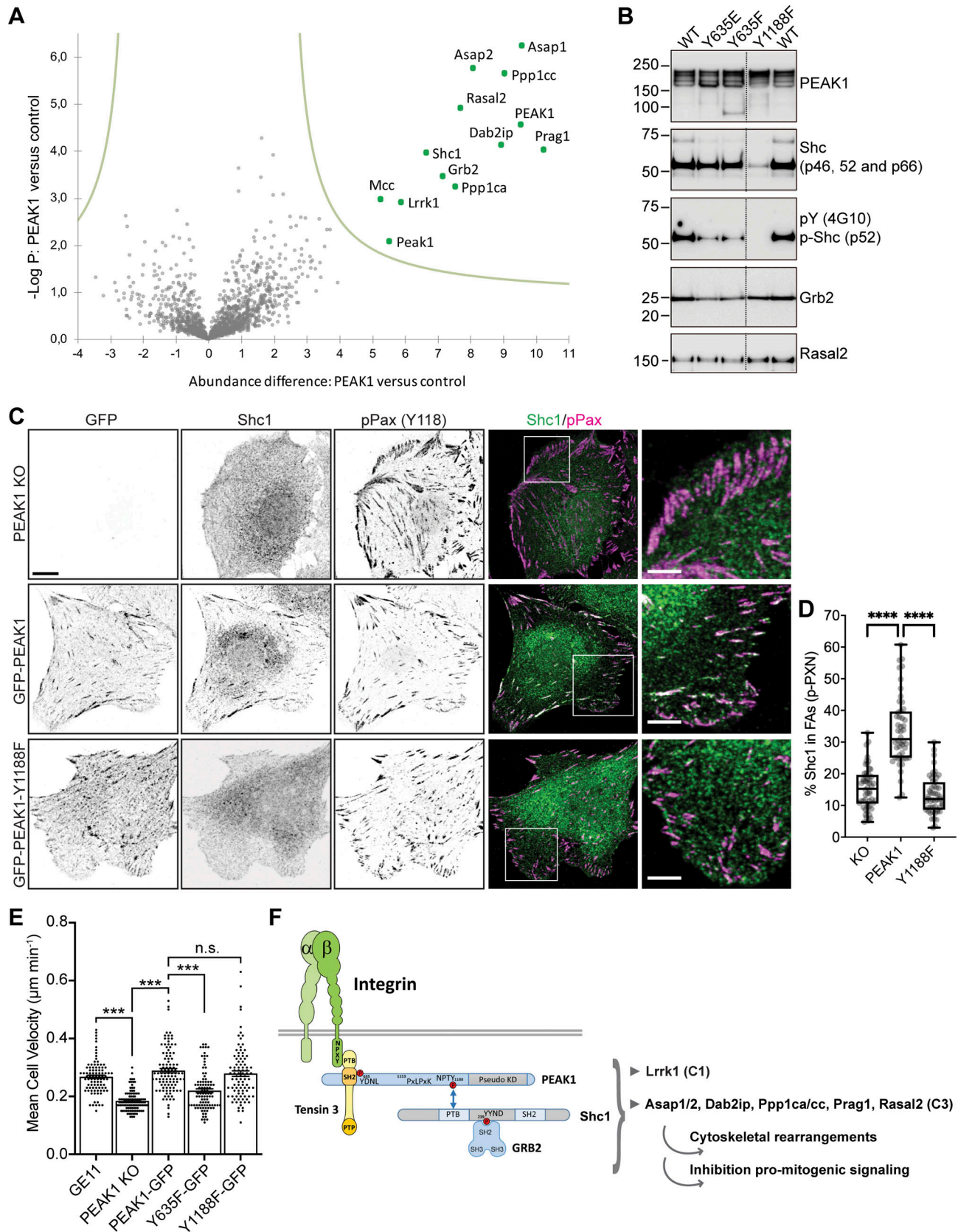


Figure 5. **PEAK1 recruits Shc1 to FAs.** (A) GFP-PEAK1 was expressed in PEAK1-deficient GE11 cells to perform GFP-TRAP experiments followed by MS analysis of binding partners. Volcano plot shows proteins enriched in PEAK1-GFP over control (PEAK1 knockout cells) samples. The logarithmic ratio of protein LFQs were plotted against negative logarithmic P values of a two-sided two-sample t test. The hyperbolic curve separates significantly enriched proteins (indicated in green) from common binders (FDR: 0.05,  $n = 4$ ). (B) GFP-PEAK1 WT or Y635E/Y635F/Y1188F mutants were expressed in PEAK1-deficient GE11

cells. Representative Western blots of GFP-TRAP experiments are shown. **(C)** Colocalization of GFP-PEAK1, Shc1 (green in merge), and Paxillin (magenta in merge) in PEAK1-deficient versus GFP-PEAK1 WT or Y1188F mutant-expressing GE11 cells. Scale bar, 10  $\mu\text{m}$ ; in magnified regions, 5  $\mu\text{m}$ . **(D)** Quantifications of colocalization of Shc1 and phospho-Y118 Paxillin (calculated as a percentage of total Shc1) of immunofluorescence images as shown in C.  $n = 3$ , total number of cells analyzed: 52 (KO); 48 (PEAK1); 51 (Y1188F). Box plots range from the 25th to 75th percentile; central line indicates the median; whiskers show smallest to largest value. Mann-Whitney  $U$  test was performed to determine statistical significance. \*\*\*\*,  $P < 0.0001$ . **(E)** Migration of GE11 Tet-ON integrin  $\beta 1$  cells (WT or PEAK1-deficient with or without rescue with the indicated PEAK1-GFP constructs) treated with 1  $\mu\text{g}/\text{ml}$  doxycycline for 48 h to induce  $\beta 1$  expression on fibronectin-coated plastic was analyzed in overnight videos. Kruskal-Wallis with Dunn's multiple comparisons test was performed to determine statistical significance; error bars show SEM; \*\*\*,  $P < 0.0001$ ;  $n = 93$  (GE11), 105 (PEAK1 KO), 105 (PEAK1-GFP), 94 (PEAK1-Y635F), 94 (PEAK1-Y1188F) cells. **(F)** Model of PEAK1 and its binding partners. PEAK1 is connected to integrins by Tensin3, which binds to phospho-Y635 PEAK1 and the integrin  $\beta$  MP-NPXY motif. Shc1 binds phospho-Y1188 PEAK1. PEAK1 also interacts with proteins that were classified in different clusters based on their association rates with Shc1 upon EGF stimulation (Zheng et al., 2013), including the cluster 1 (C1) proteins Grb2 and Lrrk1 and C3 proteins Asap1/2, Dab2ip, Ppp1ca/cc, Prag1, and Rasal2. Source data are available for this figure: SourceData F5.

(Zheng et al., 2013) and recruits Shc1 to FAs by interacting with Tensin3 and RGD-binding integrins (Fig. 5 F). Moreover, integrins and growth factor receptors synergize to regulate cellular functions, including cell motility (Miyamoto et al., 1996; Morello et al., 2011). In line with these findings, expression of PEAK1-Y635F, which showed decreased binding to tyrosine-phosphorylated Shc1, was unable to restore the migration velocity of GE11 PEAK1 KO cells, unlike expression of PEAK1 WT (Fig. 5 E). PEAK1 could be an important player in regulating integrin-growth factor receptor synergism, as it connects RGD-binding integrins to the protein cluster regulating late EGFR/Shc1 signaling (Zheng et al., 2013).

## Materials and methods

### Antibodies

Primary antibodies used are listed in Table S6. Secondary antibodies were as follows: goat anti-rabbit Alexa Fluor 488, goat anti-mouse Alexa Fluor 488, goat anti-mouse Texas Red, goat anti-mouse Alexa Fluor 568, donkey anti-rabbit Alexa Fluor 594, goat anti-rabbit Alexa Fluor 647, and goat anti-mouse Alexa Fluor 647 (Invitrogen); PE-conjugated donkey anti-rabbit antibody (#406421; BioLegend); and stabilized goat anti-mouse HRP-conjugated and stabilized goat anti-rabbit HRP-conjugated (Pierce; Bio-Rad).

### Generation of phospho-site-specific Y365 PEAK1 antibodies

The phospho-peptide KVPIVINPNAY(PO3H2)DNLAIFYKS with a cysteine added at the C-terminus was synthesized. The phospho-peptide was chemically conjugated with mariculture keyhole limpet hemocyanin (mcKLH) using Imject Maleimide-Activated mcKLH Spin Kit (77666; Thermo Fisher Scientific) according to the manufacturer's protocol. Briefly, 1 mg phospho-peptide dissolved in 500  $\mu\text{l}$  conjugation buffer was mixed with 2 mg mcKLH dissolved in water for 2 h at room temperature, and the conjugate was desalted and collected by passing through the Zeba Spin Desalting Column. Two rabbits were immunized with 500  $\mu\text{g}$  mcKLH-conjugated peptide in TiterMax Gold-Adjuvant (T2684; Sigma-Aldrich) and subsequently boosted with the same mcKLH conjugated phospho-peptide in Freund's incomplete adjuvant (F5506; Sigma-Aldrich) at 4, 8, and 12 wk. After the final immunization, blood of the animals was collected, and IgG was purified on a Protein A Sepharose column (Pharmacia LKB Biotechnology). The phospho-specific antibodies were then purified by positive and negative affinity purification. For positive

affinity purification, the phosphorylated peptide was covalently coupled to SulfoLink Coupling Gels from Pierce according to the manufacturer's protocol. Bound antibodies were eluted with 1 M glycine-HCl, pH 2.9, and neutralized with an equal volume of 1 M Tris-HCl, pH 8.5. Protein-containing fractions were pooled and concentrated with Amicon Ultra-4 10K centrifugal filter devices (Millipore). After washing with PBS using the same filter devices, the concentrated protein fraction was added to a second column in which the corresponding nonphosphorylated peptide was covalently bound. All flow-through fractions containing antibodies were collected and stored at 4°C.

### Cell lines

GE11  $\beta 1$  null cells were isolated from  $\beta 1$  chimeric embryos, as previously described (Gimond et al., 1999). SW480 and U251MG cell lines were obtained from American Type Culture Collection. COS-7 cells have been described previously (De Melker et al., 1997). All cell lines were cultured in DMEM containing 10% heat-inactivated FBS and antibiotics. All cells were cultured at 37°C in a humidified, 5%  $\text{CO}_2$  atmosphere.

### Generation of PEAK1-deficient cells

The target sgRNA against mouse *Peak1* (exon 4; 5'-AAGCAATTC TTGCATTCGCCAGG-3') or human *PEAK1* (exon 4; 5'-TGCCCG TGTTCTGATGCGG-3') was cloned into pX330-U6-Chimeric\_BB-CBh-hSpCas9 (a kind gift from Feng Zhang, Broad Institute of MIT and Harvard, Cambridge, MA [Cong et al., 2013]; plasmid #42230; Addgene). GE11 cells were transfected with this vector in combination with a blasticidin cassette, as previously described (Heijink et al., 2015), and selected with 4  $\mu\text{g}/\text{ml}$  blasticidin (Sigma-Aldrich) for 4 d after transfection. Transfected SW480 cells were selected with 2.5  $\mu\text{g}/\text{ml}$  puromycin for 3 d.

### Stable cellular transduction

The integrin  $\beta 1$  (mutants), generated as previously described (Margadant et al., 2012), were subcloned into the EcoRI and BamHI sites of the pcDNA3.1 MCS-BirA(R118G)-HA vector (a gift from Kyle Roux [plasmid #36047; Addgene; Roux et al., 2012]). The integrin  $\alpha 3$ -BirA\* construct was cloned by 3-point ligation of an N-terminal PCR fragment containing an EcoRI site and a C-terminal part of 2.3 kb into EcoRI and BamHI sites of the pcDNA3.1 MCS-BirA(R118G)-HA vector. The integrin  $\alpha 5$ -BirA\* construct was cloned by 3-point ligation of a N-terminal part

of 2.7 kb and a C-terminal PCR fragment lacking the stop codon into the BamHI site of the pcDNA3.1 MCS-BirA(R118G)-HA vector. The integrin  $\alpha$ 6-BirA\* construct was described previously (Te Molder et al., 2020). The integrin  $\beta$ 1-BirA\* (mutants),  $\alpha$ 5-BirA\*,  $\alpha$ 3-BirA\*, and  $\alpha$ 6-BirA\* constructs were cloned into the SnaBI site of the LZRS-IRES-Zeo vector.

The pRetroX-DSRed-SGK269 plasmid encoding human PEAK1 cDNA was kindly provided by Dr. Roger Daly. The PEAK1 construct was subcloned by 3-point ligation of a N-terminal part of 4.9 kb and a C-terminal PCR fragment creating a stop codon and NotI site into EcoRI and NotI sites of pUC19 vector. Point mutants of PEAK1 Y635E, Y635F, and Y1188F were generated by site-directed mutagenesis with the PCR-based overlap extension method using Pfu DNA polymerase (Promega) and subcloned into the EcoRI and NotI sites of the pLZRS-EGFP vector, as previously described (Ketema et al., 2013).

Retroviral vectors were introduced into Phoenix packaging cells using the calcium phosphate method. Virus-containing supernatant was collected 48 h later. After retroviral transduction, infected cells were selected with 0.2 mg/ml zeocin (Invitrogen).

#### Generation of stable knockdown cell lines

Short hairpins against human Tensin3 (cloned into pLKO.1) were obtained from the MISSION TRC shRNA collection and transfected into HEK 293FT cells using Lipofectamine 2000 (Invitrogen). U251MG  $\beta$ 5-BirA\*-expressing cells were generated as previously described (Zuidema et al., 2018), infected with the produced recombinant lentivirus, and selected with puromycin for 3 d. Target sequences included: 5'-CCGGACGCATAGGAG TGGTCATATCCTCGAGGATATGACCACTCCTATGCGTTTTTTG-3' (shRNA 1) and 5'-CCGGCTCCAGCAAAGCGTTCAAACCTCGA GGTTTGAACGCTTTGCTGGGAGTTTTTTG-3' (shRNA 4).

#### Transient transfection

Talin1 (M-040902-01-0020), Talin2 (M-065877-01-0020), Filamin-A (M-058520-02-0020), and Filamin-C (M-055631-01-0020) siGENOME SMARTpool siRNAs were purchased from Dharmacon. GE11 cells were transiently transfected using lipofectamine 2000 (Invitrogen). Lipofectamine (20  $\mu$ l/ml) and siRNA (0.5  $\mu$ M) solutions in Opti-MEM were mixed (1:1) and incubated for 30 min at room temperature. Cells were incubated with the transfection solution overnight.

#### Flow cytometry

Cells were treated as indicated, trypsinized, and washed twice in PBS containing 2% FCS, followed by primary antibody (1:200 dilution) incubation for 1 h at 4°C. Then, cells were washed three times in PBS containing 2% FCS and incubated with secondary PE-conjugated antibodies (1:200 dilution) for 1 h at 4°C. After subsequent washing steps, desired cell populations were isolated by FACS sorting using a Becton Dickinson FACSAria IIu or Beckman Coulter MoFlo Astrios cell sorter.

#### BioID assay

Cells stably expressing the integrin subunit-BirA\* fusion proteins were grown on 100-mm or 3  $\times$  145-mm plates (for Western

blot or MS, respectively). Plates were coated with a laminin-332-rich matrix obtained by growing RAC-11P cells (Delwel et al., 1994) to complete confluence, after which the plates were washed with PBS and incubated with 20 mM EDTA in PBS overnight at 4°C. The RAC-11P cells were then removed by extensive washing with PBS.

Cells were washed in cold PBS, lysed in radioimmunoprecipitation assay buffer (20 mM Tris-HCl, pH 7.5, 100 mM NaCl, 4 mM EDTA, pH 7.5, 1% NP-40, 0.1% SDS, and 0.5% sodium deoxycholate) supplemented with a protease inhibitor cocktail (Sigma-Aldrich), and cleared by centrifugation at 14,000 *g* for 30 min at 4°C. Lysates were incubated with Streptavidin Sepharose High Performance beads (GE Healthcare) overnight at 4°C. Beads were washed three times with NP40 buffer (20 mM Tris-HCl, pH 7.5, 100 mM NaCl, 4 mM EDTA, pH 7.5, and 1% NP-40) and twice with PBS, and the isolated biotinylated proteins were analyzed by MS or Western blotting.

#### GFP pull-down assays

Cells were washed in cold PBS, lysed in NP40 lysis buffer (20 mM Tris-HCl, pH 7.5, 100 mM NaCl, 4 mM EDTA, pH 7.5, and 1% NP-40) supplemented with a protease inhibitor cocktail (Sigma-Aldrich), 1.5 mM Na<sub>3</sub>VO<sub>4</sub>, and 15 mM NaF (Cell Signaling Technology), and cleared by centrifugation at 14,000 *g* for 30 min at 4°C. Lysates were incubated with GFP-Trap Agarose (Chromotek) according to the manufacturer's instructions. Beads were washed three times with NP-40 lysis buffer and twice with PBS, and the isolated proteins were analyzed by MS or Western blotting.

#### GST pull-down assay and Western blotting

COS-7 cells were cotransfected with plasmids expressing GST and GST fusion proteins of Tensin3 WT (SH2-WT) and SH2-domain mutants (SH2-2F; Y1206F/Y1256F and SH2-3F; Y173F/Y1206F/Y1256; a kind gift from Douglas Lowy [Qian et al., 2009]), and a PEAK1 expressing plasmid using the DEAE-Dextran method (De Melker et al., 1997). 2 d after transfection, the cells were treated with or without pervanadate and lysed in NP-40 lysis buffer. After clearance of the lysates by centrifugation, equal amounts of proteins were used for pull-down assays by adding 25  $\mu$ l glutathione Sepharose 4B beads (GE-Healthcare) and rotating for 4 h at 4°C. The beads were washed three times with NP-40 lysis buffer and two times with PBS, and bound proteins were eluted with Laemmli sample buffer containing 2%  $\beta$ -mercaptoethanol at 95°C for 5 min. Proteins were separated by electrophoresis using Bolt Novex 4–12% gradient Bis-Tris gels (Invitrogen), transferred to Immobilon-P transfer membranes (Millipore Corp.), and blocked for  $\geq$ 30 min in 2% BSA in TBST buffer (10 mM Tris, pH 7.5, 150 mM NaCl, and 0.3% Tween-20). Primary antibody (diluted 1:1,000 in 2% BSA in TBST buffer) incubation took place overnight at 4°C. After washing twice with TBST and twice with TBS buffer, blots were incubated for 1 h at room temperature with HRP-conjugated goat anti-mouse IgG or goat anti-rabbit IgG (diluted 1:3,000 in 2% BSA in TBST buffer). After subsequent washing steps, the bound antibodies were detected by enhanced chemiluminescence using SuperSignal West Dura Extended Duration Substrate (Thermo

Fisher Scientific) or Clarity Western ECL Substrate (Bio-Rad) as described by the manufacturer. Signal intensities were quantified using ImageJ.

## MS

For BioID experiments, peptide mixtures were prepared, measured, and analyzed as previously described (Wang et al., 2020), with the following exceptions. Peptide mixtures (33% of total digest) were loaded directly on the analytical column and analyzed by nanoLC-MS/MS on an Orbitrap Fusion Tribrid mass spectrometer equipped with a Proxeon nLC1200 system (Thermo Fisher Scientific). Solvent A was 0.1% formic acid/water and solvent B was 0.1% formic acid/80% acetonitrile. Peptides were eluted from the analytical column at a constant flow of 250 nl/min in a 115-min gradient, containing a 100-min linear increase from 5 to 24% solvent B, followed by a 15-min wash at 90% solvent B.

Raw data were analyzed by MaxQuant (v2.0.1.0; Cox et al., 2014) using standard settings for label-free quantitation (LFQ). MS/MS data were searched against the *Mus musculus* Swissprot database (17,082 entries, release 2021\_07) complemented with a list of common contaminants and concatenated with the reversed version of all sequences. LFQ intensities were  $\log_2$ -transformed in Perseus (v1.6.15.0; Tyanova et al., 2016), after which proteins were filtered for at least three valid values (of four total). Differentially expressed proteins were determined using Student's *t* test (threshold: false discovery rate [FDR]: 5% and S0: 0.1).

GFP pull-down samples were loaded on an SDS-PAGE gel. Gel bands were excised into  $\sim 1 \times 1$ -mm pieces and subjected to destaining and reduction alkylation of cysteines, followed by overnight digestion with Trypsin (Promega). After digestion, the peptides were desalted and concentrated via StageTips. Peptides were separated on a 40-min gradient on a 15-cm analytical column (75  $\mu$ m inner diameter) packed with 1.9  $\mu$ m ReproSil Gold C18 reversed phase particles (Dr. Maisch). The column was maintained at 50°C, and peptides were directly sprayed into a Q Exactive HF mass spectrometer via a nano-electrospray ionization source. The mass spectrometer was operated in data-dependent mode, and  $\leq 15$  precursors were selected for fragmentation. Raw data were processed using MaxQuant (v1.6.0.15), and all identifications were filtered at 1% FDR.

## Immunofluorescence

Subconfluent cells were fixed with 2% PFA for 10 min, permeabilized with 0.2% Triton X-100 for 5 min, and blocked with PBS containing 2% BSA (Sigma-Aldrich) for  $\geq 30$  min. Next, cells were incubated with the primary antibodies for 1 h at room temperature. Cells were washed three times before incubation with the secondary antibodies for 1 h. Additionally, the nuclei were stained with DAPI, and F-actin was visualized using Alexa Fluor 488- or 647-conjugated phalloidin (BioLegend; AAT Bioquest). After three washing steps with PBS, the coverslips were mounted onto glass slides in Mowiol. Images were obtained at room temperature using a Leica TCS SP5 confocal microscope with a AOBS scan head (158001107; Leica), controlled using Leica LAS AF SP5 software (v2.7.4), with a 63 $\times$ /1.4 Oil CS HC PL APO objective (11506350; Leica), with filter cubes for 488/eGFP (15525302; Leica), 568/mCherry (15525303; Leica), and DAPI (15525301; Leica).

## Cell motility

GE11 Tet-ON integrin  $\beta 1$  cells (WT, PEAK1 KO, and PEAK1 KO stably expressing PEAK1-GFP, PEAK1-Y635F-GFP, or PEAK1-Y1188F-GFP) were cultured for  $\geq 48$  h with 1  $\mu$ g/ml doxycycline to induce  $\beta 1$  integrin expression, and then plated onto fibronectin-coated (10  $\mu$ g/ml in PBS) plastic 12-well plates (20,000 cells per well) in DMEM containing 0.5% FBS, antibiotics, and doxycycline (1  $\mu$ g/ml). After culture overnight, the medium was exchanged for DMEM containing 0.5% FBS, antibiotics, and doxycycline (1  $\mu$ g/ml), and cells were transferred to the heated stage (37°C with 5% CO<sub>2</sub>) of a Zeiss AxioObserver Z.1 microscope. Phase-contrast images were acquired with a 10 $\times$ /0.30 EC Plan-Neofluar Ph1 objective (Zeiss), captured with a Zeiss AxioCam MRm. Images were acquired every 10 min for 20 h. Cells were tracked manually using ImageJ; tracking data were analyzed using the Chemotaxis Tool plugin (Ibidi).

## Image analysis and statistical analysis

Image analysis was performed using Fiji (ImageJ; Schindelin et al., 2012; Schneider et al., 2012). To quantify Shc1 clustering in FAs (based on Paxillin staining), background was subtracted in both channels using a bilateral filter, and the region of interest was selected at the cell periphery. Colocalization of Shc1 and FAs was determined using the Image Calculator (command "multiply") on both channels and calculating the area of overlapping fraction as a percentage of the total Shc1 area per cell using the Analyze Particle function. The amount of GFP-PEAK1 (WT or Y635F) present in FAs was calculated in the same manner, using vinculin staining as a marker for FAs.

Mann-Whitney *U* test (two-tailed *P* value) was performed using GraphPad Prism (v7.0c). In figures, statistically significant values are shown as \*\*\*\*, *P* < 0.0001. Graphs were made in GraphPad Prism and show all data points. Data distribution was assumed to be normal but was not formally tested.

## Online supplemental material

Fig. S1, a table of proteins identified as interactors of both integrin  $\beta 1$  and  $\beta 3$  in the BioID experiments, shows surface expression of the integrin BirA\* constructs, assessed using FACS. Fig. S2 is related to data showing that PEAK1 is recruited to Tensin3 at cell matrix adhesions via a process requiring phosphorylation driven by Src. Fig. S3 shows interactors of GFP-PEAK from GFP-Trap-based affinity purification followed by MS in cells treated with EGF. Tables S1, S2, S3, S4 and S5 are Excel files with the MS data for proximity interactors of Integrin  $\beta 1$ -BirA\* (Table S1, complete data; Table S2, top 60 interactors), Integrin  $\beta 3$ -BirA\* (Table S3, complete data; Table S4, top 60 interactors), and GFP-Trap based affinity purification MS of GFP-PEAK expressed in PEAK1-null SW480 cells (Table S5). Table S6 is a list of antibodies used in this study.

## Acknowledgments

We thank Anne Cress (University of Arizona Cancer Center, Tucson, AZ), David Critchley (University of Leicester, Leicester, UK), Roger Daly (Monash University, Victoria, Australia), Marina Glukhova (Institut Curie, PSL Research University, CNRS, Paris,

France), Simon Goodman (Merck KGaA, Darmstadt, Germany), Douglas Lowy (National Institutes of Health, Bethesda, MD), Jacques Neefjes (Leiden University Medical Centre, Leiden, The Netherlands), Ellen van der Schoot (Sanquin Research, Amsterdam, The Netherlands), and NKI colleagues for sharing cells and reagents.

This work was supported by the Dutch Cancer Society (project 12143). Liesbeth Hoekman and Onno B. Bleijerveld are supported by the Dutch NWO X-omics Initiative. A. Sonnenberg and R. Fässler thank the Alexander von Humboldt Foundation for supporting A. Sonnenberg during his sabbatical year at the Max-Planck Institute.

The authors declare no competing financial interests.

Author contributions: A. Zuidema and A. Sonnenberg conceived the study, designed experiments, interpreted data, and wrote the manuscript with contributions from P. Atherton. A. Zuidema, P. Atherton, M. Kreft, L. Hoekman, O.B. Bleijerveld, N. Nagaraj, N. Chen, and A. Sonnenberg performed and analyzed the experiments. R. Fässler provided resources and reviewed and edited the manuscript.

Submitted: 5 August 2021

Revised: 22 March 2022

Accepted: 18 May 2022

## References

Abu-Thuraia, A., M.A. Goyette, J. Boulais, C. Delliaux, C. Apcher, C. Schott, R. Chidiac, H. Bagci, M.P. Thibault, D. Davidson, et al. 2020. AXL confers cell migration and invasion by hijacking a PEA1-regulated focal adhesion protein network. *Nat. Commun.* 11:3586. <https://doi.org/10.1038/s41467-020-17415-x>

Agajanian, M., A. Campeau, M. Hoover, A. Hou, D. Brambilla, S.L. Kim, R.L. Klemke, and J.A. Kelber. 2015. PEA1 acts as a molecular switch to regulate context-dependent TGF $\beta$  responses in breast cancer. *PLoS One*. 10:e0135748. <https://doi.org/10.1371/journal.pone.0135748>

Bouchet, B.P., R.E. Gough, Y.C. Ammon, D. van de Willige, H. Post, G. Jacquemet, A.M. Altelaar, A.J. Heck, B.T. Goult, and A. Akhmanova. 2016. Talin-KANK1 interaction controls the recruitment of cortical microtubule stabilizing complexes to focal adhesions. *Elife*. 5:e18124. <https://doi.org/10.7554/eLife.18124>

Bristow, J.M., T.A. Reno, M. Jo, S.L. Gonias, and R.L. Klemke. 2013. Dynamic phosphorylation of tyrosine 665 in pseudopodium-enriched atypical kinase 1 (PEAK1) is essential for the regulation of cell migration and focal adhesion turnover. *J. Biol. Chem.* 288:123–131. <https://doi.org/10.1074/jbc.M112.410910>

Calderwood, D.A., Y. Fujioka, J.M. de Pereda, B. Garcia-Alvarez, T. Nakamoto, B. Margolis, C.J. McGlade, R.C. Liddington, and M.H. Ginsberg. 2003. Integrin beta cytoplasmic domain interactions with phosphotyrosine-binding domains: A structural prototype for diversity in integrin signaling. *Proc. Natl. Acad. Sci. USA*. 100:2272–2277. <https://doi.org/10.1073/pnas.262791999>

Cao, X., T. Kaneko, J.S. Li, A.D. Liu, C. Voss, and S.S. Li. 2015. Erratum: A phosphorylation switch controls the spatiotemporal activation of rho GTPases in directional cell migration. *Nat. Commun.* 6:8320. <https://doi.org/10.1038/ncomms9320>

Charrin, S., S. Jouannet, C. Boucheix, and E. Rubinstein. 2014. Tetraspanins at a glance. *J. Cell Sci.* 127:3641–3648. <https://doi.org/10.1242/jcs.154906>

Chastney, M.R., C. Lawless, J.D. Humphries, S. Warwood, M.C. Jones, D. Knight, C. Jorgensen, and M.J. Humphries. 2020. Topological features of integrin adhesion complexes revealed by multiplexed proximity biotinylation. *J. Cell Biol.* 219:e202003038. <https://doi.org/10.1083/jcb.202003038>

Chumbalkar, V., K. Latha, Y. Hwang, R. Maywald, L. Hawley, R. Sawaya, L. Diao, K. Baggerly, W.K. Cavenee, F.B. Furnari, and O. Bogler. 2011. Analysis of phosphotyrosine signaling in glioblastoma identifies STAT5 as a novel downstream target of  $\Delta$ EGFR. *J. Proteome Res.* 10:1343–1352. <https://doi.org/10.1021/pr101075e>

Cong, L., F.A. Ran, D. Cox, S. Lin, R. Barretto, N. Habib, P.D. Hsu, X. Wu, W. Jiang, L.A. Marraffini, and F. Zhang. 2013. Multiplex genome engineering using CRISPR/Cas systems. *Science*. 339:819–823. <https://doi.org/10.1126/science.1231143>

Cowan, K.J., D.A. Law, and D.R. Phillips. 2000. Identification of shc as the primary protein binding to the tyrosine-phosphorylated beta 3 subunit of alpha IIb beta 3 during outside-in integrin platelet signaling. *J. Biol. Chem.* 275:36423–36429. <https://doi.org/10.1074/jbc.M004068200>

Cox, J., M.Y. Hein, C.A. Luber, I. Paron, N. Nagaraj, and M. Mann. 2014. Accurate proteome-wide label-free quantification by delayed normalization and maximal peptide ratio extraction, termed MaxLFQ. *Mol. Cell. Proteomics*. 13:2513–2526. <https://doi.org/10.1074/mcp.M113.031591>

Croucher, D.R., F. Hochgrafe, L. Zhang, L. Liu, R.J. Lyons, D. Rickwood, C.M. Tactacan, B.C. Browne, N. Ali, H. Chan, et al. 2013. Involvement of Lyn and the atypical kinase Sgk269/PEAK1 in a basal breast cancer signaling pathway. *Cancer Res.* 73:1969–1980. <https://doi.org/10.1158/0008-5472.CAN-12-1472>

Cui, Y., Y.C. Liao, and S.H. Lo. 2004. Epidermal growth factor modulates tyrosine phosphorylation of a novel tensin family member, Tensin3. *Mol. Cancer Res.* 2:225–232. <https://doi.org/10.1158/1541-7786.225.2.4>

De Melker, A.A., D. Kramer, I. Kuikman, and A. Sonnenberg. 1997. The two phenylalanines in the GFFKR motif of the integrin alpha6A subunit are essential for heterodimerization. *Biochem. J.* 328:529–537. <https://doi.org/10.1042/bj3280529>

Delwel, G.O., A.A. de Melker, F. Hogervorst, L.H. Jaspars, D.L. Fles, I. Kuikman, A. Lindblom, M. Paulsson, R. Timpl, and A. Sonnenberg. 1994. Distinct and overlapping ligand specificities of the alpha 3A beta 1 and alpha 6A beta 1 integrins: Recognition of laminin isoforms. *Mol. Biol. Cell.* 5:203–215. <https://doi.org/10.1091/mbc.5.2.203>

Deshmukh, L., V. Gorbatyuk, and O. Vinogradova. 2010. Integrin {beta}3 phosphorylation dictates its complex with the Shc phosphotyrosine-binding (PTB) domain. *J. Biol. Chem.* 285:34875–34884. <https://doi.org/10.1074/jbc.M110.159087>

Ding, C., W. Tang, X. Fan, X. Wang, H. Wu, H. Xu, W. Xu, W. Gao, and G. Wu. 2018. Overexpression of PEA1 contributes to epithelial-mesenchymal transition and tumor metastasis in lung cancer through modulating ERK1/2 and JAK2 signaling. *Cell Death Dis.* 9:802. <https://doi.org/10.1038/s41419-018-0817-1>

Dong, J.M., F.P.-L. Tay, H.L.-F. Swa, J. Gunaratne, T. Leung, B. Burke, and E. Manser. 2016. Proximity biotinylation provides insight into the molecular composition of focal adhesions at the nanometer scale. *Sci. Signal.* 9:rs4. <https://doi.org/10.1126/scisignal.aaf3572>

Fujimura, K., T. Wright, J. Strnadel, S. Kaushal, C. Metildi, A.M. Lowy, M. Bouvet, J.A. Kelber, and R.L. Klemke. 2014. A hypusine-eIF5A-PEAK1 switch regulates the pathogenesis of pancreatic cancer. *Cancer Res.* 74:6671–6681. <https://doi.org/10.1158/0008-5472.CAN-14-1031>

Geiger, B., and K.M. Yamada. 2011. Molecular architecture and function of matrix adhesions. *Cold Spring Harbor Perspect. Biol.* 3:a005033. <https://doi.org/10.1101/cshperspect.a005033>

Gimond, C., A. van Der Flier, S. van Delft, C. Brakebusch, I. Kuikman, J.G. Collard, R. Fässler, and A. Sonnenberg. 1999. Induction of cell scattering by expression of beta1 integrins in beta1-deficient epithelial cells requires activation of members of the rho family of GTPases and down-regulation of cadherin and catenin function. *J. Cell Biol.* 147:1325–1340. <https://doi.org/10.1083/jcb.147.6.1325>

Ha, B.H., and T.J. Boggon. 2018. The crystal structure of pseudokinase PEA1 (Sugen kinase 269) reveals an unusual catalytic cleft and a novel mode of kinase fold dimerization. *J. Biol. Chem.* 293:1642–1650. <https://doi.org/10.1074/jbc.RA117.000751>

Heijink, A.M., V.A. Blomen, X. Bisteau, F. Degener, F.Y. Matsushita, P. Kaldis, F. Foijer, and M.A. van Vugt. 2015. A haploid genetic screen identifies the G1/S regulatory machinery as a determinant of Wee1 inhibitor sensitivity. *Proc. Natl. Acad. Sci. USA*. 112:15160–15165. <https://doi.org/10.1073/pnas.1505283112>

Horton, E.R., A. Byron, J.A. Askari, D.H.J. Ng, A. Millon-Fremillon, J. Robertson, E.J. Koper, N.R. Paul, S. Warwood, D. Knight, et al. 2015. Definition of a consensus integrin adhesome and its dynamics during adhesion complex assembly and disassembly. *Nat. Cell Biol.* 17:1577–1587. <https://doi.org/10.1038/ncb3257>

Horton, E.R., J.D. Humphries, J. James, M.C. Jones, J.A. Askari, and M.J. Humphries. 2016. The integrin adhesome network at a glance. *J. Cell Sci.* 129:4159–4163. <https://doi.org/10.1242/jcs.192054>

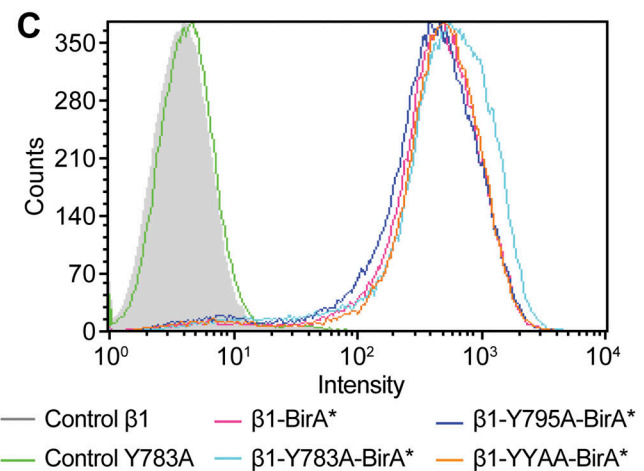
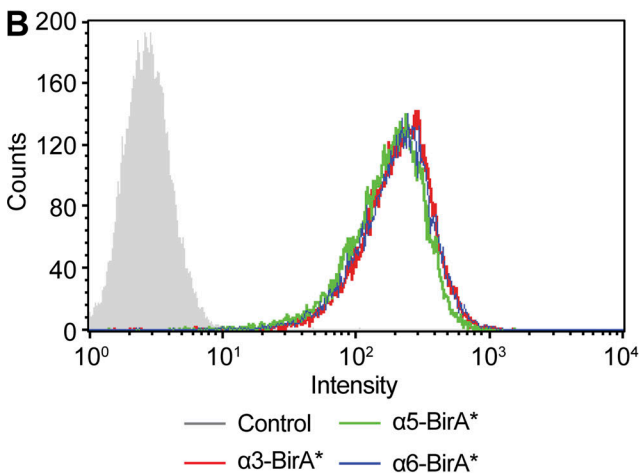
Hou, J., E.V. Nguyen, M. Surudo, M.J. Roy, O. Patel, I.S. Lucet, X. Ma, and R.J. Daly. 2022. Distinct PEA3 interactors and outputs expand the signaling potential of the PEA3 pseudokinase family. *Sci. Signal.* 15:eabj3554. <https://doi.org/10.1126/scisignal.abj3554>

- Humphries, J.D., A. Byron, M.D. Bass, S.E. Craig, J.W. Pinney, D. Knight, and M.J. Humphries. 2009. Proteomic analysis of integrin-associated complexes identifies RCC2 as a dual regulator of Rac1 and Arf6. *Sci. Signal.* 2: ra51. <https://doi.org/10.1126/scisignal.2000396>
- Hynes, R.O. 2002. Integrins: Bidirectional, allosteric signaling machines. *Cell.* 110:673–687. [https://doi.org/10.1016/s0092-8674\(02\)00971-6](https://doi.org/10.1016/s0092-8674(02)00971-6)
- Kelber, J.A., T. Reno, S. Kaushal, C. Metildi, T. Wright, K. Stoletov, J.M. Weems, F.D. Park, E. Mose, Y. Wang, et al. 2012. KRas induces a Src/PEAK1/ErbB2 kinase amplification loop that drives metastatic growth and therapy resistance in pancreatic cancer. *Cancer Res.* 72:2554–2564. <https://doi.org/10.1158/0008-5472.CAN-11-3552>
- Ketema, M., M. Krefl, P. Secades, H. Janssen, and A. Sonnenberg. 2013. Nesprin-3 connects plectin and vimentin to the nuclear envelope of Sertoli cells but is not required for Sertoli cell function in spermatogenesis. *Mol. Biol. Cell.* 24:2454–2466. <https://doi.org/10.1091/mbc.E13-02-0100>
- Kiema, T., Y. Lad, P. Jiang, C.L. Oxley, M. Baldassarre, K.L. Wegener, I.D. Campbell, J. Ylance, and D.A. Calderwood. 2006. The molecular basis of filamin binding to integrins and competition with talin. *Mol. Cell.* 21: 337–347. <https://doi.org/10.1016/j.molcel.2006.01.011>
- Leroy, C., C. Fialin, A. Sirvent, V. Simon, S. Urbach, J. Poncet, B. Robert, P. Jouin, and S. Roche. 2009. Quantitative phosphoproteomics reveals a cluster of tyrosine kinases that mediates SRC invasive activity in advanced colon carcinoma cells. *Cancer Res.* 69:2279–2286. <https://doi.org/10.1158/0008-5472.CAN-08-2354>
- Liao, Y.C., L. Si, R.W. deVere White, and S.H. Lo. 2007. The phosphotyrosine-independent interaction of DLC-1 and the SH2 domain of cten regulates focal adhesion localization and growth suppression activity of DLC-1. *J. Cell Biol.* 176:43–49. <https://doi.org/10.1083/jcb.200608015>
- Manninen, A., and M. Varjosalo. 2017. A proteomics view on integrin-mediated adhesions. *Proteomics.* 17. <https://doi.org/10.1002/pmic.201600022>
- Margadant, C., M. Krefl, D.J. de Groot, J.C. Norman, and A. Sonnenberg. 2012. Distinct roles of talin and kindlin in regulating integrin  $\alpha 5\beta 1$  function and trafficking. *Curr. Biol.* 22:1554–1563. <https://doi.org/10.1016/j.cub.2012.06.060>
- Mauro, L., D. Sisci, M. Bartucci, M. Salerno, J. Kim, T. Tam, M.A. Guvakova, S. Ando, and E. Surmacz. 1999. SHC- $\alpha 5\beta 1$  integrin interactions regulate breast cancer cell adhesion and motility. *Exp. Cell Res.* 252: 439–448. <https://doi.org/10.1006/excr.1999.4639>
- McCleverty, C.J., D.C. Lin, and R.C. Liddington. 2007. Structure of the PTB domain of tensin1 and a model for its recruitment to fibrillar adhesions. *Protein Sci.* 16:1223–1229. <https://doi.org/10.1110/ps.072798707>
- Miyamoto, S., H. Teramoto, J.S. Gutkind, and K.M. Yamada. 1996. Integrins can collaborate with growth factors for phosphorylation of receptor tyrosine kinases and MAP kinase activation: Roles of integrin aggregation and occupancy of receptors. *J. Cell Biol.* 135:1633–1642. <https://doi.org/10.1083/jcb.135.6.1633>
- Morello, V., S. Cabodi, S. Sigismund, M.P. Camacho-Leal, D. Repetto, M. Volante, M. Papotti, E. Turco, and P. Defilippi. 2011.  $\beta 1$  integrin controls EGFR signaling and tumorigenic properties of lung cancer cells. *Oncogene.* 30:4087–4096. <https://doi.org/10.1038/ncr.2011.107>
- Morse, E.M., N.N. Brahme, and D.A. Calderwood. 2014. Integrin cytoplasmic tail interactions. *Biochemistry.* 53:810–820. <https://doi.org/10.1021/bi401596q>
- Moser, M., K.R. Legate, R. Zent, and R. Fassler. 2009. The tail of integrins, talin, and kindlins. *Science.* 324:895–899. <https://doi.org/10.1126/science.1163865>
- Ng, D.H., J.D. Humphries, A. Byron, A. Millon-Fremillon, and M.J. Humphries. 2014. Microtubule-dependent modulation of adhesion complex composition. *PLoS One.* 9:e115213. <https://doi.org/10.1371/journal.pone.0115213>
- Patel, O., M.D.W. Griffin, S. Panjekar, W. Dai, X. Ma, H. Chan, C. Zheng, A. Kropp, J.M. Murphy, R.J. Daly, and I.S. Lucet. 2017. Structure of Sgk223 pseudokinase reveals novel mechanisms of homotypic and heterotypic association. *Nat. Commun.* 8:1157. <https://doi.org/10.1038/s41467-017-01279-9>
- Patel, O., M.J. Roy, J.M. Murphy, and I.S. Lucet. 2020. The PEAK family of pseudokinases, their role in cell signalling and cancer. *FEBS J.* 287: 4183–4197. <https://doi.org/10.1111/febs.15087>
- Qian, X., G. Li, W.C. Vass, A. Papageorge, R.C. Walker, L. Asnaghi, P.J. Steinbach, G. Tosato, K. Hunter, and D.R. Lowy. 2009. The Tensin3 protein, including its SH2 domain, is phosphorylated by Src and contributes to tumorigenesis and metastasis. *Cancer Cell.* 16:246–258. <https://doi.org/10.1016/j.ccr.2009.07.031>
- Robertson, J., G. Jacquemet, A. Byron, M.C. Jones, S. Warwood, J.N. Selley, D. Knight, J.D. Humphries, and M.J. Humphries. 2015. Defining the phospho-adhesome through the phosphoproteomic analysis of integrin signalling. *Nat. Commun.* 6:6265. <https://doi.org/10.1038/ncomms7265>
- Roux, K.J., D.I. Kim, M. Raida, and B. Burke. 2012. A promiscuous biotin ligase fusion protein identifies proximal and interacting proteins in mammalian cells. *J. Cell Biol.* 196:801–810. <https://doi.org/10.1083/jcb.201112098>
- Schiller, H.B., C.C. Friedel, C. Boulegue, and R. Fassler. 2011. Quantitative proteomics of the integrin adhesome show a myosin II-dependent recruitment of LIM domain proteins. *EMBO Rep.* 12:259–266. <https://doi.org/10.1038/embor.2011.5>
- Schiller, H.B., M.R. Hermann, J. Polleux, T. Vignaud, S. Zanivan, C.C. Friedel, Z. Sun, A. Raducanu, K.E. Gottschalk, M. Thery, et al. 2013.  $\beta 1$ - and  $\alpha$ -class integrins cooperate to regulate myosin II during rigidity sensing of fibronectin-based microenvironments. *Nat. Cell Biol.* 15:625–636. <https://doi.org/10.1038/ncb2747>
- Schindelin, J., I. Arganda-Carreras, E. Frise, V. Kaynig, M. Longair, T. Pietzsch, S. Preibisch, C. Rueden, S. Saalfeld, B. Schmid, et al. 2012. Fiji: An open-source platform for biological-image analysis. *Nat. Methods.* 9: 676–682. <https://doi.org/10.1038/nmeth.2019>
- Schneider, C.A., W.S. Rasband, and K.W. Eliceiri. 2012. NIH image to ImageJ: 25 years of image analysis. *Nat. Methods.* 9:671–675. <https://doi.org/10.1038/nmeth.2089>
- Smith, M.J., W.R. Hardy, J.M. Murphy, N. Jones, and T. Pawson. 2006. Screening for PTB domain binding partners and ligand specificity using proteome-derived NPXY peptide arrays. *Mol. Cell. Biol.* 26:8461–8474. <https://doi.org/10.1128/MCB.01491-06>
- Strnadel, J., S. Choi, K. Fujimura, H. Wang, W. Zhang, M. Wyse, T. Wright, E. Gross, C. Peinado, H.W. Park, et al. 2017. eIF5A-PEAK1 signaling regulates YAP1/TAZ protein expression and pancreatic cancer cell growth. *Cancer Res.* 77:1997–2007. <https://doi.org/10.1158/0008-5472.CAN-16-2594>
- Sun, Z., H.Y. Tseng, S. Tan, F. Senger, L. Kurazawa, D. Dedden, N. Mizuno, A.A. Wasik, M. Thery, A.R. Dunn, and R. Fassler. 2016. Kank2 activates talin, reduces force transduction across integrins and induces central adhesion formation. *Nat. Cell Biol.* 18:941–953. <https://doi.org/10.1038/ncb3402>
- Te Molder, L., L. Hoekman, M. Krefl, O. Bleijerveld, and A. Sonnenberg. 2020. Comparative interactomics analysis reveals potential regulators of  $\alpha 6\beta 4$  distribution in keratinocytes. *Biol. Open.* 9:bio054155. <https://doi.org/10.1242/bio.054155>
- Tyanova, S., T. Temu, P. Sinitcyn, A. Carlson, M.Y. Hein, T. Geiger, M. Mann, and J. Cox. 2016. The Perseus computational platform for comprehensive analysis of (prote)omics data. *Nat. Methods.* 13:731–740. <https://doi.org/10.1038/nmeth.3901>
- Wang, W., A. Zuidema, L. Te Molder, L. Nahidiazar, L. Hoekman, T. Schmidt, S. Coppola, and A. Sonnenberg. 2020. Hemidesmosomes modulate force generation via focal adhesions. *J. Cell Biol.* 219:e201904137. <https://doi.org/10.1083/jcb.201904137>
- Wang, Y., J.A. Kelber, H.S. Tran Cao, G.T. Cantin, R. Lin, W. Wang, S. Kaushal, J.M. Bristow, T.S. Edgington, R.M. Hoffman, et al. 2010. Pseudopodium-enriched atypical kinase 1 regulates the cytoskeleton and cancer progression [corrected]. *Proc. Natl. Acad. Sci. USA.* 107:10920–10925. <https://doi.org/10.1073/pnas.0914776107>
- Wary, K.K., F. Mainiero, S.J. Isakoff, E.E. Marcantonio, and F.G. Giancotti. 1996. The adaptor protein Shc couples a class of integrins to the control of cell cycle progression. *Cell.* 87:733–743. [https://doi.org/10.1016/s0092-8674\(00\)81392-6](https://doi.org/10.1016/s0092-8674(00)81392-6)
- Wavreille, A.S., and D. Pei. 2007. A chemical approach to the identification of tensin-binding proteins. *ACS Chem. Biol.* 2:109–118. <https://doi.org/10.1021/cb600433g>
- Winograd-Katz, S.E., R. Fassler, B. Geiger, and K.R. Legate. 2014. The integrin adhesome: From genes and proteins to human disease. *Nat. Rev. Mol. Cell Biol.* 15:273–288. <https://doi.org/10.1038/nrm3769>
- Yam, J.W.P., F.C.F. Ko, C.Y. Chan, D.-Y. Jin, and I.O.-L. Ng. 2006. Interaction of deleted in liver cancer 1 with tensin2 in caveolae and implications in tumor suppression. *Cancer Res.* 66:8367–8372. <https://doi.org/10.1158/0008-5472.CAN-05-2850>
- Zaidel-Bar, R., S. Itzkovitz, A. Ma'ayan, R. Iyengar, and B. Geiger. 2007. Functional atlas of the integrin adhesome. *Nat. Cell Biol.* 9:858–867. <https://doi.org/10.1038/ncb0807-858>
- Zheng, Y., C. Zhang, D.R. Croucher, M.A. Soliman, N. St-Denis, A. Pasculescu, L. Taylor, S.A. Tate, W.R. Hardy, K. Colwill, et al. 2013. Temporal regulation of EGF signalling networks by the scaffold protein Shc1. *Nature.* 499:166–171. <https://doi.org/10.1038/nature12308>
- Zuidema, A., W. Wang, M. Krefl, L. Te Molder, L. Hoekman, O.B. Bleijerveld, L. Nahidiazar, H. Janssen, and A. Sonnenberg. 2018. Mechanisms of integrin  $\alpha V\beta 5$  clustering in flat clathrin lattices. *J. Cell Sci.* 131:jcs221317. <https://doi.org/10.1242/jcs.221317>

## Supplemental material

**A**

Uniprot Accession	Gene Name	Description	Uniprot Accession	Gene Name	Description
P26039	Tln1	Talin-1	Q8CDJ8	Ston1	Stonin-1
P43406	Itgav	Integrin alpha-V	B9EJ80	Pdzd8	PDZ domain-containing protein 8
Q69ZN7	Myof	Myoferlin	Q61029	Tmpo	Lamina-associated polypeptide 2, isoforms $\beta$ , $\delta$ , $\epsilon$ , $\gamma$
Q69Z38	Peak1	Pseudopodium-enriched atypical kinase 1	Q8BQZ4	Ralgapb	Ral GTPase-activating protein subunit beta
Q80UU9	Pgmc2	Membrane-associated progesterone receptor component 2	P18572	Bsg	Basigin
Q91WL8	Wwox	WW domain-containing oxidoreductase	P32507	Pvr12	Nectin-2
Q8K1S3	Unc5b	Netrin receptor UNC5B	Q9D0F3	Lman1	Protein ERGIC-53
O54890	Itgb3	Integrin beta-3	Q71LX4	Tln2	Talin-2
Q811D0	Dlg1	Disks large homolog 1	Q3UR85	Myrf	Myelin regulatory factor
F8VQB6	Myo10	Unconventional myosin-X	Q5DTU0	Afap1l2	Actin filament-associated protein 1-like 2
Q5SYH2	Tmem199	Transmembrane protein 199	Q03145	Epha2	Ephrin type-A receptor 2
O70318	Epb41l2	Band 4.1-like protein 2	Q9QY76	Vapb	Vesicle-associated membrane protein-associated protein B
Q99P72	Rtn4	Reticulon-4	O09044	Snap23	Synaptosomal-associated protein 23
Q9WTQ5	Akap12	A-kinase anchor protein 12	Q99KW3	Triobp	TRIO and F-actin-binding protein
Q8C1B7	Septin11	Septin-11	Q8CIN4	Pak2	Serine/threonine-protein kinase PAK 2
P70302	Stim1	Stromal interaction molecule 1	Q9Z0U1	Tjp2	Tight junction protein ZO-2
Q8BX02	Kank2	KN motif and ankyrin repeat domain-containing protein 2	Q9DBR4	Appb2	Amyloid beta A4 precursor protein-binding family B member 2
Q62407	Speg	Striated muscle-specific serine/threonine-protein kinase	Q9VW55	Vapa	Vesicle-associated membrane protein-associated protein A
P56395	Cyb5a	Cytochrome b5	Q3UMF0	Cobl1	Cordon-bleu protein-like 1
Q6P9J9	Ano6	Anoctamin-6	Q9EPE9	Atp13a1	Manganese-transporting ATPase 13A1
Q9Z2B5	Eif2ak3	Eukaryotic translation initiation factor 2-alpha kinase 3	Q5SSZ5	Tns3	Tensin-3
P47740	Aldh3a2	Fatty aldehyde dehydrogenase	Q9VWC3	Cav2	Caveolin-2
O70252	Hmox2	Heme oxygenase 2	Q5FWI3	Tmem2	Transmembrane protein 2
Q8CIB5	Fermt2	Fermitin family homolog 2	Q6P1H6	Ankle2	Ankyrin repeat and LEM domain-containing protein 2



**D**

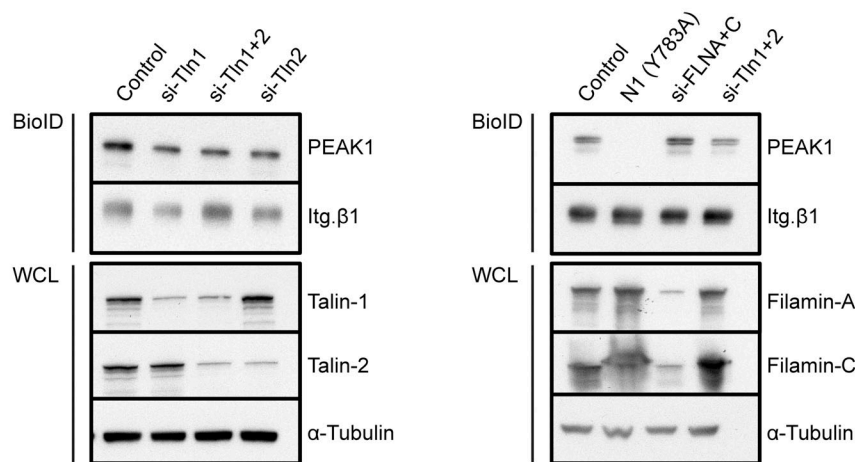
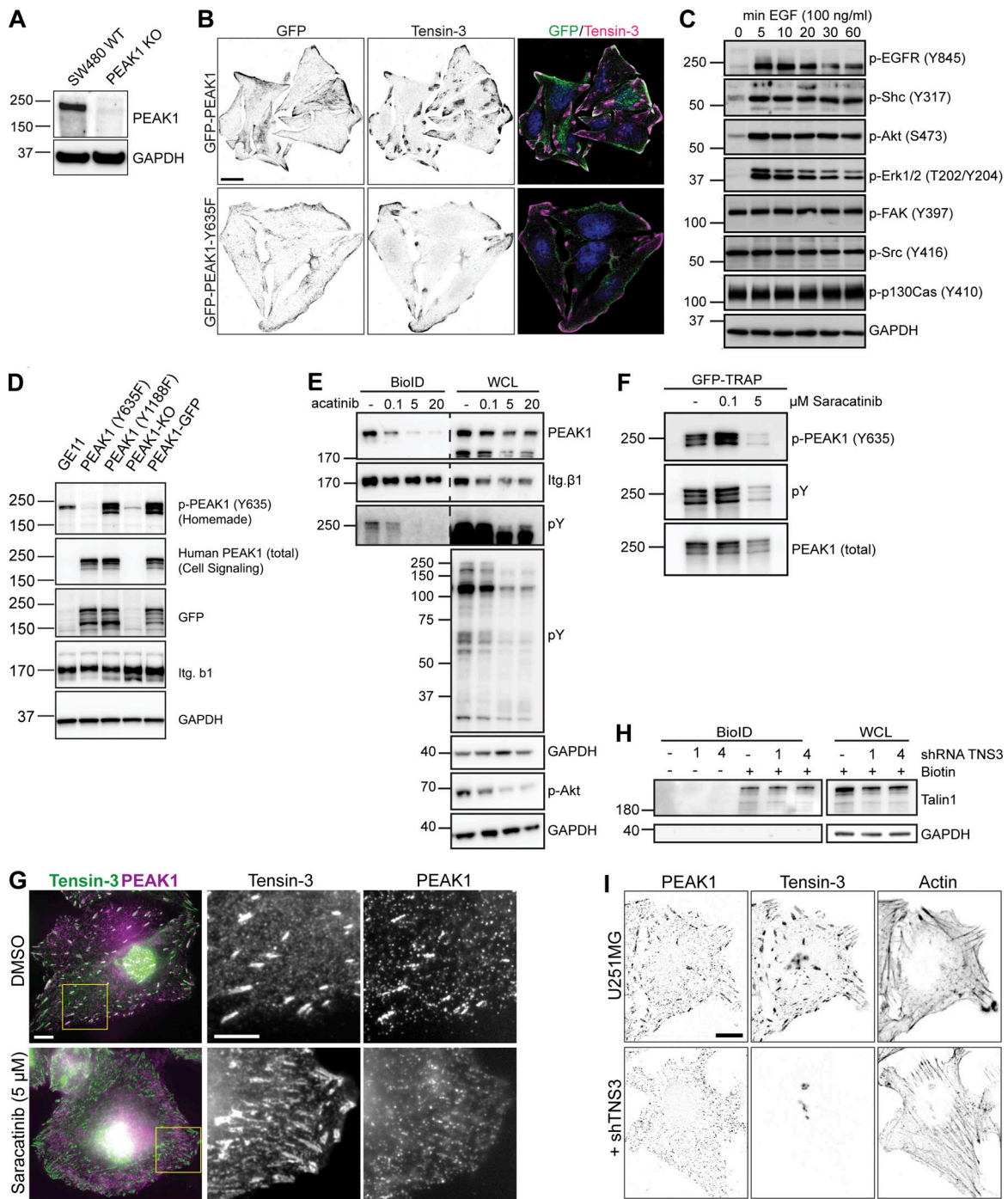


Figure S1. **Identification of overlapping proteins in  $\beta$ 1- and  $\beta$ 3-BioID data sets, expression of integrin subunits and knockdown of integrin NPxY-binding proteins.** (A) Table of proteins identified in both the integrin  $\beta$ 1-BirA\* and integrin  $\beta$ 3-BirA\* BioID datasets. (B and C) Flow cytometry analyses of Itg.  $\beta$ 1 expression in GE11 cells stably expressing the indicated integrin  $\alpha$  (B) or mutant  $\beta$ 1 (C) subunits with a C-terminal BirA\* tag. (D) Western blots of BioID assays performed using GE11/ $\beta$ 1-BirA\* cells transfected with siRNAs against Talin1/2 or Filamin A/C 72 h before cell lysis. All samples were treated with 50  $\mu$ M biotin 24 h before cell lysis. WCL, whole-cell lysate. Source data are available for this figure: SourceData FS1.



**Figure S2. Biochemical and immunofluorescent analysis of Tensin3-PEAK1 interactions.** (A) SW480 WT or PEAK1 KO (generated using CRISPR/Cas9) cells were lysed and analyzed by Western blot for PEAK1 expression. (B) SW480 PEAK1 KO cells stably expressing GFP-PEAK1 or GFP-PEAK1-Y635F cultured overnight on coverslips before fixation and staining for Tensin3; scale bar, 10  $\mu$ m. (C) GE11 cells expressing GFP-PEAK1 were serum starved for 16 h and treated with 50 ng/ml EGF for the indicated periods of time. Phosphorylation of indicated proteins was analyzed by Western blot. (D) Lysates of GE11 cells (GE11) and PEAK1-deficient GE11 cells (KO) reconstituted with GFP-PEAK1 (WT) or the GFP-PEAK1 mutants (Y635F and Y1188F) were analyzed by Western blot with antibodies against phospho-PEAK1 (Y365; homemade), total PEAK1, GFP,  $\beta$ 1 integrin, or GAPDH. (E) Representative Western blots of BioID assays performed using GE11/ $\beta$ 1-BirA\* cells treated with different concentrations of the Src inhibitor Saracatinib (AZD0530) for 24 h. (F) GFP-PEAK1 was expressed in PEAK1-deficient GE11 cells, and cells were treated with Saracatinib as indicated for 24 h before cell lysis. Subsequently, GFP pull-downs were performed, and PEAK1 Y635 phosphorylation was analyzed by Western blot. (G) U251MG cells spread on fibronectin-coated coverslips overnight with either Saracatinib (5  $\mu$ M) or an equivalent volume of DMSO were fixed and stained for Tensin3 and PEAK1. Note the absence of PEAK1 from Tensin3 positive adhesion structures in Src inhibited cells. Scale bar, 10  $\mu$ m. (H) Representative Western blots of BioID assays performed using integrin  $\beta$ 5-deficient U251MG cells expressing  $\beta$ 5-BirA\*, in which Tensin3 was depleted by two different shRNAs (1 and 4). Cells were treated with 50  $\mu$ M biotin 24 h before cell lysis. WCL, whole-cell lysate. (I) U251MG cells transfected with control or shRNA against TNS3 were fixed and stained for PEAK1 and Tensin3. Note the lack of PEAK1 at cell matrix adhesions in shTNS3 cells. Scale bar, 10  $\mu$ m. Source data are available for this figure: SourceData FS2.

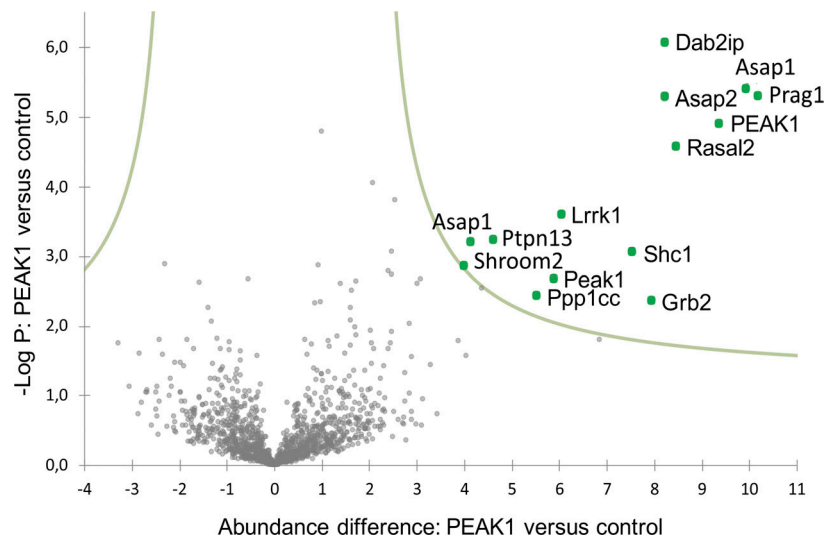


Figure S3. **PEAK1 interactome of EGF stimulated GE11 cells.** PEAK1-deficient GE11 cells expressing GFP-PEAK1 were treated with EGF for 20 min, lysed, and subjected to immunoprecipitation using GFP-TRAP. Volcano plot shows proteins enriched in PEAK1-GFP over control (PEAK1 knockout cells) samples. The logarithmic ratios of protein LFQs were plotted against negative logarithmic P values of a two-sided two-sample t test. The hyperbolic curve separates significantly enriched proteins (indicated in green) from common binders (FDR: 0.05,  $n = 4$ ).

Provided online are Table S1, Table S2, Table S3, Table S4, Table S5, and Table S6. Table S1 is a complete list of  $\beta$ 1 proximity interactors by BioID. Table S2 shows the top 60 hits of  $\beta$ 1 proximity interactors by BioID. Table S3 is a complete list of  $\beta$ 3 proximity interactors by BioID. Table S4 shows the top 60 hits of  $\beta$ 3 proximity interactors by BioID. Table S5 shows mass spectrometry analysis of GFP-PEAK1 associated proteins. Table S6 lists antibodies used in this study.